



GEM-MACH-PAH (rev2488): a new high-resolution chemical transport model for North American PAHs and benzene

Cynthia H. Whaley^{1,2}, Elisabeth Galarneau¹, Paul A. Makar¹,
Ayodeji Akingunola¹, Wanmin Gong¹, Sylvie Gravel¹, Michael D. Moran¹,
Craig Stroud¹, Junhua Zhang¹, and Qiong Zheng¹

¹Air Quality Research Division, Environment and Climate Change Canada, 4905 Dufferin Street,
Toronto, ON, M3H 5T4, Canada

²Climate Research Division, Environment and Climate Change Canada, 4905 Dufferin Street,
Toronto, ON, M3H 5T4, Canada

Correspondence to: Cynthia Whaley (cynthia.whaley@canada.ca)

Abstract. Environment and Climate Change Canada's online air quality forecasting model, GEM-MACH, was extended to simulate atmospheric concentrations of benzene and seven polycyclic aromatic hydrocarbons (PAHs): phenanthrene, anthracene, fluoranthene, pyrene, benz(a)anthracene, chrysene, and benzo(a)pyrene. In the expanded model, benzene and PAHs are emitted from major point, area, and mobile sources, with emissions based on recent emission factors. Modelled PAHs undergo gas-particle partitioning (whereas benzene is only in the gas phase), atmospheric transport, oxidation, cloud processing, and dry and wet deposition. To represent PAH gas-particle partitioning, the Dachs-Eisenreich scheme was used, and we have improved gas-particle partitioning parameters based on an empirical analysis to get significantly better gas-particle partitioning results than the previous North American PAH model, AURAMS-PAH. Other added process parameterizations include the particle phase benzo(a)pyrene reaction with ozone via the Kwamena scheme and gas-phase scavenging of PAHs by snow via vapor sorption to the snow surface.

The resulting GEM-MACH-PAH model was used to generate the first online model simulations of PAH emissions, transport, chemical transformation and deposition for a high resolution domain (2.5-km grid cell spacing) in North America, centered on the PAH-data-rich region of southern Ontario, Canada and the north-eastern United States. Model output for two seasons was compared to measurements from three monitoring networks spanning Canada and the U.S. Average summertime model results were found to be statistically indistinguishable from measurements of benzene and all seven PAHs. The same was true for the winter seasonal mean, except for benzo(a)pyrene (BaP), which had a statistically significant positive bias. We present evidence that the benzo(a)pyrene results may be ameliorated via further improvements to PM and oxidant processes and transport. Our analysis focused on four key components to the prediction of atmospheric PAH levels: spatial variability; sensitivity to mobile emissions; gas-particle partitioning; and wet deposition. Spatial variability of



PAHs/PM_{2.5} at 2.5-km resolution was found to be comparable to measurements. Predicted ambient
25 surface concentrations of benzene and the PAHs were found to be critically dependent on mobile
emission factors, indicating the mobile emissions sector has a significant influence on ambient PAH
levels in the study region. PAH wet deposition was overestimated due to additive precipitation biases
in the model and the measurements. Our overall performance evaluation suggests that GEM-MACH-
PAH can provide seasonal estimates for benzene and PAHs and be suitable for emissions scenario
30 simulations.

1 Introduction

Polycyclic aromatic hydrocarbons (PAHs) are semi-volatile atmospheric pollutants that have numer-
ous negative health effects (some are carcinogenic, mutagenic, and teratogenic) (Kim et al., 2013).
Measurements of PAHs in North America are sparse in both time (typically 24-hour averages, every 6
35 days) and space (limited surface measurement networks), yet show ambient concentrations that reg-
ularly exceed the Ontario provincial government's health-based threshold (Galarneau et al., 2016).
Similarly, benzene is a gas-phase single-ring aromatic hydrocarbon, is a known carcinogen, and
also exceeds atmospheric health-based guidelines (Galarneau et al., 2016). Accurate, 3-dimensional
40 modelling of PAHs and benzene can fill in the space-time gaps of the measurements, identify atmo-
spheric processes that are responsible for the threshold exceedances, and simulate effects of emis-
sions scenarios.

AURAMS (A Unified Regional Air quality Modelling System) was an offline (meteorology from
a weather forecast model used as an input), Eulerian 3-D chemical transport model (CTM) de-
veloped by Environment and Climate Change Canada (ECCC). In Galarneau et al. (2014), AU-
45 RAMS was modified to include seven PAH species (phenanthrene, anthracene, fluoranthene, pyrene,
benz(a)anthracene, chrysene, and benzo(a)pyrene – hereafter abbreviated to PHEN, ANTH, FLRT,
PYR BaA, CHRY, BaP, respectively). AURAMS-PAH included emissions, transport, gas-particle
partitioning, oxidation of the gas-phase PAHs with OH, dry deposition, and wet deposition of the
particle-phase PAHs. This model was able to accurately simulate the 2002 annual average PAH
50 concentrations in North America when compared to 45 measurement sites, located in Ontario,
the north-eastern U.S., and California. However, the AURAMS-PAH gas-particle partitioning over-
predicted the gas phase for the lighter PAH species, and was employed at relatively poor time and
spatial resolutions. It was also missing two known PAH loss processes: the surface reaction of O₃
on particulate BaP (Kwamena et al., 2004, 2007; Ringuet et al., 2012; Keyte et al., 2013; Liu et al.,
55 2014), and snow scavenging of gas-phase PAHs (Franz and Eisenreich, 1998; Daly and Wania, 2004;
Lei and Wania, 2004; Skrdlíková et al., 2011). These missing processes, along with the coarse (42-
km) spatial resolution, may have contributed to the differences between model results and measure-



ments. Also, this model used PAH emission factors for mobile emissions which are now out-of-date for representing the modern vehicle fleet.

60 Other PAH CTMs include GEOS-Chem (Friedman and Selin, 2012; Thackray et al., 2015), which is a global model, CMAQ, which was run on the Europe continental domain in Aulinger et al. (2007), and in North America in Zhang et al. (2016, 2017), FARM (Flexible Air quality Regional Model) (Gariazzo et al., 2007), which is a regional model, applied for the region of Rome, Italy, and WRF-Chem-PAH (Mu et al., 2017), which modelled East Asia. The most relevant of these model studies
65 to our own is the one by Zhang et al. (2016, 2017), whereby they ran CMAQ with 16 PAH species added, at 36-km resolution in a mainly U.S. domain (that included parts of Canada and Mexico), evaluated their model results against NATTS measurements, and used their results to determine cancer risk to U.S. human populations from various sources.

Therefore, the goal of this study is to update and improve ECCC's PAH modelling capabilities by
70 using a more advanced model framework, updating emission inventories, and utilizing better process representation of PAHs than were used in AURAMS-PAH to allow better exploration of PAH processes and scenarios. To achieve this goal, GEM-MACH (Global Environment Multiscale model – Modelling Air quality and CHemistry), ECCC's next generation, online air quality forecasting model (meteorology and air-quality are predicted in the same code) was modified to include the same seven
75 PAH species, as well as benzene. PAH processes parameterization were improved in the following ways: 1. On-road mobile PAH emissions were updated with more recent data, to better represent the modern vehicle fleet; 2. gas-particle partitioning parameters were improved based on empirical results and analysis of AURAMS model output; 3. process representation for the on-particle O₃ - particulate BaP reaction was added to the model; and 4. process representation for in- and below-
80 cloud wet scavenging (including scavenging by snow) were added for gas-phase PAHs and benzene. Simulations using GEM-MACH-PAH were then carried out at high (2.5-km) spatial resolution in a small, but densely populated North American domain including southern Ontario, and most of the northeastern U.S. (Fig. 1) for summer and winter of 2009. We refer to this region as the "Pan Am" domain because it was created for high-resolution air quality modelling during the 2015 Pan American Games in Ontario (Joe et al., 2017). This domain contains approximately 109 million people, including about 38% of the Canadian population and 30% of the U.S. population. The model results were evaluated using measurements from a high-spatial-resolution campaign in Hamilton, Ontario (Anastasopoulos et al., 2012), as well as the binational Integrated Atmospheric Deposition Network (IADN), the Canadian National Air Pollution Surveillance network (NAPS), and the U.S. National
85 Air Toxics Trends Stations network (NATTS). We focus our model evaluation on spatial variations at high resolution, estimating the level of model sensitivity to uncertainties in the PAH emission factors, gas-particle partitioning, and wet deposition, which are all related to novel aspects of the GEM-MACH-PAH model.



The following sections will further describe the GEM-MACH-PAH model (Section 2), the mea-
95 surements used for evaluation (Section 3), the results of the model evaluation (Section 4), and con-
clusions (Section 5).

2 Model Description

In the present study, we have modified ECCC's high-resolution air quality forecasting model, GEM-
MACH (hereafter called "GEM-MACH-PAH"), to include benzene and seven PAHs (in both gas
100 and particle-phases) and have carried out 6 months of simulations in 2009 at the highest resolution
(2.5-km grid cell size) in a North American domain yet reported for PAH simulations, to our knowl-
edge. We have also tracked PAH wet deposition, and gas-particle partitioning, and have attempted to
qualify model sensitivity to uncertainty in mobile emission factors, which has not been reported in
other model studies.

105 2.1 GEM-MACH overview

GEM-MACH is an on-line, 3D chemical transport model, which is embedded in GEM, ECCC's
operational numerical weather prediction model (Côté et al., 1998b, a; Moran et al., 2010). On-line
models such as GEM-MACH improve air-quality chemical prediction performance by reducing in-
terpolation errors between different model coordinate systems and removing the input/output time
110 and disk storage required for the transfer of meteorological input files to their off-line CTM coun-
terparts (e.g., Baklanov et al., 2014). The coupling to meteorology is a one-way process in this ver-
sion, whereby chemistry does not influence the meteorology. More detailed description of the gas-,
aqueous-, and particle-phase process representations of GEM-MACH, and an evaluation of its per-
formance for common pollutants such as ozone, particulate matter (PM), and ammonia appears in
115 Moran et al. (2013); Makar et al. (2015b, a); Gong et al. (2015), and Whaley et al. (2017). Here we
will focus on the model changes made to include PAH species and processes.

GEM-MACH is used to provide ECCC's twice-daily, 48-hour operational public forecasts of crite-
ria air pollutants (ozone, nitrogen oxides, PM), as well as the Air Quality Health Index [<https://ec.gc.ca/cas-aqhi/>].
To reduce the computational burden for forecasting, the PM size distribution is represented using a
120 simplified sectional treatment consisting of two size bins, a fine-fraction bin for particles with Stokes
diameter from 0 to 2.5 μm and a coarse-fraction bin for particles with Stokes diameter from 2.5 to 10
 μm (Moran et al., 2010), with sub-binning used for those particle processes requiring a finer particu-
late size distribution. Here, we utilize the research version of GEM-MACH version 2, revision 2476,
with this two-size-bin representation as our starting point for PAH modifications. The model grid
125 used corresponds to a rotated latitude-longitude map projection with 2.5-km horizontal grid spacing
and a hybrid vertical coordinate with 80-level vertical discretization spanning the atmosphere from
the surface to 0.1 hPa.



2.2 Model modifications for benzene and PAH species

Our modifications to GEM-MACH include adding benzene and seven gas-phase and 14 particle-
 130 phase (7 species \times 2 size bins) PAHs to the species arrays, and adding the gas-particle partitioning
 subroutine described in Galarneau et al. (2014), but with updated partitioning parameters (see Sec-
 tion 2.2.1). Since PAHs have very small concentrations relative to criteria air contaminants, as in
 Galarneau et al. (2014), we assume they do not have a significant effect on oxidant concentrations
 (O_3 and OH). Thus, the PAHs in GEM-MACH-PAH make use of the outcomes of the model's gas
 135 and aqueous-phase chemistry in a diagnostic fashion for PAH oxidation. Processes in which the
 PAHs participate directly include advection, vertical diffusion, plume rise of major point source
 emissions, aerosol particle microphysics, in- and below-cloud scavenging, and dry and wet depo-
 sition of both gas and particle phases. Some of these processes and/or their controlling param-
 eters were updated relative to Galarneau et al. (2014) and are described in the subsections below.
 140 Like AURAMS-PAH, the total (gas+particle) PAH emissions were treated as gas-phase emissions
 in GEM-MACH-PAH, since these quickly repartition between particles and gas phases following
 emission. The non-PAH and PAH emissions are described further below.

2.2.1 Gas-particle partitioning

As PAHs are semi-volatile organic compounds that partition between the particulate and gaseous
 145 phases of the atmosphere, their partitioning is a major determinant of their atmospheric fate (Bidleman,
 1988). Despite decades of study (Junge, 1977; Yamasaki et al., 1982; Bidleman and Foreman, 1987;
 Pankow, 1987; Smith and Harrison, 1996; Dachs and Eisenreich, 2000; Lohmann and Lammel, 2004;
 Keyte et al., 2013), the mechanisms responsible for PAH partitioning and its spatiotemporal variabil-
 ity are not well-understood. AURAMS-PAH included two parametrizations to calculate gas/particle
 150 partitioning: Junge-Pankow, JP (Junge, 1977; Pankow, 1987) and Dachs-Eisenreich, DE (Dachs and Eisenreich,
 2000), both of which, when applied for partitioning in AURAMS-PAH, assigned too much PAH
 mass to the gas phase. The two schemes resulted in surprisingly similar gas-particle partition-
 ing (Galarneau et al., 2014). We carried out post-processing and analysis on the AURAMS-PAH
 model output from both schemes as well as the observations of gas and particle PAHs from the
 155 Galarneau et al. (2014) study, in order to determine which scheme to proceed with in GEM-MACH-
 PAH, and how it could be improved.

Measured PAH partitioning typically takes the linear form of:

$$\log K_{p,k} = m_K \log p_{L,k}^{\circ} + b_K, \quad (1)$$

where $K_{p,k}$ is the partitioning coefficient for each PAH species, k:

$$160 \log K_{p,k} = \log \left[\frac{C_p / C_{TSP}}{C_g} \right], \quad (2)$$



and C_p , C_{TSP} , and C_g are the concentrations of the particulate PAH, the total suspended particles, and the gas-phase PAH, respectively. $p_{L,k}^{\circ}$ is the sub-cooled liquid vapour pressure of the k 'th gas, and m_k and B_k are empirically derived coefficients. This linear relationship (where the $\log K_p$ of all PAH species in any given measurement sample fall on a line relative to their $\log p_L$) is common among homologous compound groups such as PAHs, polychlorinated biphenyls (PCBs), and polychlorinated dioxins and furans. However, the JP formulation only allows for $m_K = -1$ (see Section B in the supplemental material for more detailed information and a derivation). Conversely, observation-based estimates show a wide variety of $|m_K|$ values that are usually less than 1 (e.g., Fig. B.1a in the Supplemental Material), and this could be the reason why the AURAMS-PAH JP model results under-predicted the particulate fraction.

Therefore, we proceeded with the Dachs-Eisenreich formulation in GEM-MACH, but with improved parameters. The Dachs-Eisenreich (DE) partitioning formulation was adapted from work examining water-sediment partitioning (Dachs and Eisenreich, 2000). The DE expression for K_p (Eq. (B.2.1)) is related to the octanol-air and soot-air partitioning coefficients, the latter depending on the soot-water ($K_{SW,k}$) and air-water partitioning coefficients. The soot-water partitioning coefficients are highly uncertain. Their values in the literature span two orders of magnitude for the same compound (Dachs and Eisenreich, 2000; Bucheli and Gustafsson, 2000; Jonker and Koelmans, 2002; Xu et al., 2012). $K_{SW,k}$ from Jonker and Koelmans (2002), was used in AURAMS-PAH. However, using the 2002 measurement data and their average m_K , we have determined new $K_{SW,k}$ values based on ambient observations that improve the DE particulate fraction representation (see Section B.2 in the supplemental material for this process, and Table 1 for the original and new values). The purple boxes in Fig. 2 represent the results of the AURAMS-PAH partitioning module, making use of our new $K_{SW,k}$ values instead of the originals.

While the adjusted K_{SW} values in Table 1 are significantly different from those in the original model (based on Jonker and Koelmans (2002) as adjusted by the relative contributions of PM mass to the domain total in the inventory of Galarneau et al. (2007)), particularly for lower molecular-weight species, they fall within the range of values found in the literature [e.g., Dachs and Eisenreich, 2000; Bucheli and Gustafsson, 2000; Jonker and Koelmans, 2002; Xu et al., 2012].

2.2.2 Emissions

Chemical (non-PAH) emissions in GEM-MACH make use of data from the U.S. Environmental Protection Agency (EPA)'s 2011 National Emissions Inventory (NEI), and Canada's 2010 Air Pollutant Emission Inventory (APEI), these being the closest available inventory years to the year in which our simulations takes place (2009). PAH model emissions were created with the SMOKE emissions processing system (Sparse Matrix Operator Kernel Emissions, <https://www.cmascenter.org/smoke/>), which utilized PAH-to-TOG (total organic gases) emission factors, that were originally compiled for AURAMS-PAH by Galarneau et al. (2007, 2014). Below we outline the further modifications



and updates that we made to this existing emissions database, in order to generate updated PAH emissions for modeling.

PAH stationary emissions

200 Most of the PAH emission factors (EFs) used for the 2002 AURAMS-PAH model were compiled from the U.S. EPA's Locating and Estimating Series (U.S. EPA, 1998), AP-42 document (US EPA, 1995), and the 1999 National Emissions Inventory (NEI99), (Galarneau et al., 2007). PAH EFs for stationary sources that were published between 1999 and the present are not substantially different from those already being used in SMOKE. For example, recent literature on agricultural burning
205 (e.g., Dhammapala et al., 2007; Hall et al., 2012) reported EFs that were close (within a factor of two) to those already in the inventory. Only emissions from iron and steel production were updated to those in Odabasi et al. (2009) for electric arc furnaces, as the values used in Galarneau et al. (2007) were derived from literature published before 1990, and were 1-2 orders of magnitude larger (hence likely represented outdated (or absent) pollution control equipment).

210 *PAH mobile emissions*

On-road mobile PAH emission factors in AURAMS-PAH were taken from NEI99 (Galarneau et al., 2007). The mobile emissions in this inventory may no longer be relevant as the values compiled were from an older (1990s) vehicle fleet. Therefore, we employed updated EFs for more current on-road mobile emissions in Canada and the U.S. for 2009 modelling. Also, some off-road emissions, such
215 as emissions from helicopter and marine (large ships) were not considered before, and were added to the inventory (from Chen et al. (2006) and Agrawal et al. (2008), respectively) in this study.

MOVES 2014, the latest version of the U.S. EPA's motor vehicle emissions simulator (www.epa.gov/moves) contains a more recent standard set of mobile EFs, separated into one set of factors for gasoline vehicles, based on one large, 2008 study of vehicles in the U.S. (Sandeep et al., 2008), and one set
220 of factors for diesel vehicles, based on another large study in the U.S. (Khalek et al., 2009). In order to investigate whether these U.S. values would be representative of conditions in Canada and whether only have those two fuel-type categories are adequate, when this would neglect studies that have reported different EFs for several different vehicle/fuel categories (e.g., cars, trucks, buses, motorcycles; light- or heavy-duty; gasoline or diesel), we compiled and researched PAH-to-TOG
225 emission factors for these classes of mobile sources from over 30 recent (1999 to present) publications, as well as from the U.S. EPA's SPECIATE v4.4 database (containing data from 1990 to 2012: <https://www.epa.gov/air-emissions-modeling/speciate-version-45-through-40>). Please refer to Section C in the supplemental material for this mobile emission factor analysis. In this analysis, we found that the MOVES2014 EFs provided the best results in the model, thus they were selected for
230 use in our simulations.



2.2.3 On-particle BaP-O₃ reaction

The only PAH oxidation reactions included in AURAMS-PAH were temperature-independent OH reactions with each gas-phase PAH species (Galarneau et al., 2014), which were also added to the GEM-MACH-PAH model. Temperature-dependent OH reaction rates were not pursued because
 235 Brubaker and Hites (1998) determined that only k_{OH} for fluoranthene has a slight temperature dependence, but dependence was smaller than their error levels. Also, Friedman and Selin (2012) performed a phenanthrene sensitivity study with their model, and determined that including temperature dependence in k_{OH} did not affect their mean non-urban mid-latitude concentrations.

The AURAMS-PAH model overestimated BaP concentrations compared to measurements (Galarneau et al.,
 240 2014). This could be due to two O₃-related factors: (1) Particulate BaP measurements are known to be affected by on-filter O₃ degradation, causing measured particulate BaP measurements to be biased low (Menichini, 2009); (2) Heterogeneous BaP degradation by O₃ in ambient air (Keyte et al., 2013) was not simulated in AURAMS-PAH, thereby biasing modelled concentrations high. We therefore added a particle-phase BaP-O₃ reaction in GEM-MACH-PAH to account for the latter atmospheric
 245 process as described next. For the former, on-filter O₃ reaction, we have attempted to correct the measurements as described in Section 3.

In GEM-MACH-PAH we used the Kwamena scheme (Kwamena et al., 2004) for the atmospheric on-particle BaP-O₃ reaction, as this scheme produced the best results in Friedman and Selin (2012)'s global model, and according to our sensitivity calculations, other schemes either overestimate (e.g.,
 250 Pöschl et al., 2001) or underestimate (e.g., Kahan et al., 2006) the amount of BaP destroyed by this reaction. The Kwamena scheme was used because it produced BaP loss consistent with measurement studies (Ringuet et al., 2012; Jariyasopit et al., 2014; Liu et al., 2014). The reaction rate, k , is expressed as follows:

$$k = \frac{k_{max} K_{O_3} [O_3]}{1 + K_{O_3} [O_3]}, \quad (3)$$

255 where, $k_{max} = 0.060 \pm 0.018 \text{ s}^{-1}$ and $K_{O_3} = (2.8 \pm 1.4) \times 10^{-15} \text{ cm}^3$. The Kwamena scheme is expressed in the model as:

$$[BaP]_{reduced} = [BaP]_i e^{-k\delta t}, \quad (4)$$

where δt is the model time step in seconds. This formulation does not depend on the particle size, but rather on the overall bulk particulate concentration, and the concentration of O₃.

260 2.2.4 Dry and wet removal of PAHs and benzene

Gas-phase dry deposition follows a multiple resistance approach and single-layer "big leaf" approach (Wesely, 1989; Zhang et al., 2002; Makar et al., 2018) with a temperature dependency for Henry's Law constants and for water solubility (Sander, 1999; Ma et al., 2010). Dry deposition of benzene



and PAHs is also output by the model; however, measurements of the deposition flux of these species
265 were unavailable during the study period.

PAH particle-phase dry deposition is treated following (Zhang et al., 2001), resulting in size-
dependent particle deposition velocities.

Gas-phase benzene and PAHs undergo cloud and rain scavenging via Henry's law. Henry's law
partition coefficients (K_{AW}) for the seven PAHs is a linear relationship with inverse temperature.
270 The mass of benzene and PAHs in the gas-phase (as opposed to the aqueous phase in cloud droplets
and raindrops) is derived from:

$$K_{AW,k} = \frac{m_{gas}/V_{air}}{m_{aq}/V_{h2o}} = m_{AW}/T + b_{AW}, \quad (5)$$

and solving for m_{gas} :

$$m_{gas} = \frac{\frac{V_{air}}{V_{h2o}} K_{AW,k} m_i^{gas}}{(1 + \frac{V_{air}}{V_{h2o}} K_{AW,k})}, \quad (6)$$

275 where, m_i^{gas} is the initial mass of the gas-phase PAH before the Henry's law partitioning, and the
remaining PAH mass is scavenged to the liquid rain or cloud phases (m_{aq}). Note that Okochi et al.
(2004) reported that assuming Henry's Law equilibrium for benzene underpredicts the extent of
wet-deposition. In the absence of a suitable alternative parameterization, we used Henry's Law par-
titioning and therefore obtained a conservative estimate of wet deposition for benzene. Note that
280 benzene wet deposition is not evaluated in this paper as no measurements are available.

Where temperatures are $<0^{\circ}\text{C}$ below-cloud, or $<-15^{\circ}\text{C}$ in-cloud, scavenging of gas-phase ben-
zene and PAHs by snow and cloud-ice is done via surface adsorption following the formulation used
in Franz and Eisenreich (1998), which was also used by Wania et al. (1999); Lei and Wania (2004)
and Friedman and Selin (2012):

$$285 \quad W_g = K_{ia,k}(SA)\rho, \quad (7)$$

where W_g is the gas scavenging ratio (equal to the concentration of PAH in snow over the concen-
tration of PAH in air - both in moles/m³), $K_{ia,k}$ is the interfacial adsorption coefficient (equal to
the mass adsorbed per surface area of snow to the atmospheric vapor phase concentration - both in
ng/m³), SA is the specific surface area of the snow crystal, for which we use a constant 1 m²/g based
290 on literature values for fresh snow precipitation, which are highly variable, and for which no clear
relationship with temperature or wind speed has been found (Hoff et al., 1998; Hanot and Dominé,
1999; Domine et al., 2007; Hachikubo et al., 2014), ρ is the density of ice (0.917 g/cm³), and $K_{ia,k}$
is calculated from the following (Franz and Eisenreich, 1998):

$$\log(K_{ia,k}) = -1.2 \log p_{L,k}^{\circ} - 5.82, \quad (8)$$

295 Eq. (7) is used to determine the fraction of PAH mass in the gas and snow/cloud-ice phases.



Particle-phase PAHs are treated as passive tracers that undergo wet removal along with the modelled aerosol particles (Gong et al., 2006; Wang et al., 2010). The cloud and precipitation processes above are applied sequentially in the model using operator splitting, and the amount of PAH deposited from wet deposition is output by the model. Table D.1 in the supplemental material provides
300 all of the constants used in the model.

2.3 Model setup for two 3-month simulations

GEM-MACH-PAH, rev2488, was run from 8 May to 13 August 2009 and from 18 October 2009 to 5 January 2010, where the first week from each period is treated as a spin-up period (for chemical concentrations to stabilize and for the initial condition effects to be negligible: e.g., Samaali et al.,
305 2009), and were not used in our evaluation. The time periods were chosen to coincide with as many PAH concentration and deposition measurements as possible, while limiting simulation duration to reduce computational expenses.

The chemical initial and boundary conditions for the outer nest North American domain were taken from a one-year MOZART simulation for all pollutants (Emmons et al., 2010; Pendlebury et al.,
310 2017), except for benzene and PAHs. Initial and boundary conditions for PAHs and benzene were set to zero for the North American domain as its boundaries are generally away from PAH and benzene sources (e.g., over the ocean), and are also very distant from the Pan Am domain. The simulations for the nested Pan Am region were run using the chemical initial and boundary conditions from the 10-km North American model run.

315 The model simulation was carried out in sequence of 27-hour staggered simulations starting at 00 UTC, in order to reinitialize meteorology with the analysis at 10-km resolution. The first three hours in the 2.5-km domain were discarded as spin-up to reduce the dependency on the 10-km resolution meteorological initial conditions. Each 27-hour simulation used the chemical concentrations from the end of the previous simulation as initial conditions for the next 27 hours, and this sequence
320 continued until each 3-month period was complete.

GEM-MACH-PAH was run in the 2-size-bin mode to represent the PM size distribution, which means that particles fall in either fine mode ($PM_{2.5}$ - diameter $2.5 \mu\text{m}$ or less) or coarse mode (PM_{10} - $PM_{2.5}$ - diameter 2.5 - $10 \mu\text{m}$).

3 Measurement Description

325 We compare the GEM-MACH-PAH predictions to all of the benzene and PAH measurements available in the Pan Am domain during the two time periods in 2009. These include a high-spatial-resolution urban measurement campaign in the Hamilton, Ontario region, as well as network monitoring stations from NAPS, NATTS, and IADN. Locations of PAH and benzene measurement stations are plotted in Fig. 3 and 4a. Note that all measurement stations were *not* equipped with oxidant



330 removal technology; therefore, all measured PAHs, especially benzo(a)pyrene (which has the high-
est particulate fraction, and is the most reactive with O₃), would have had losses due to reaction
with ozone on the filters (Menichini, 2009; Liu et al., 2014), and thus would be biased low compared
to concentrations in ambient air. Accordingly, we have applied an O₃ correction to the BaP
measurements in this study, as the literature suggests that the BaP sampling artifact is substantial,
335 with around 20-72% lost on average during sampling (Menichini, 2009; Liu et al., 2014). Note that
our correction follows the linear method recommended by Schauer et al. (2003), which is dependent
only on O₃ concentrations. However, other studies state that the O₃ degradation of BaP is more
complex, with additional dependencies on the resident atmospheric lifetime of BaP (Goriaux et al.,
2006), and relative humidity (Pitts Jr. et al., 1986; Umwelterhebungen and Gerätesicherheit, 2002;
340 Menichini, 2009). However, those studies did not provide an alternative correction equation. Therefore,
in our results, we will present both the Schauer-corrected BaP measurements (for sites that had
O₃ monitors nearby), as well as the original reported BaP from the measurements, given the lack of
a better correction for the sampling artifact.

3.1 Hamilton measurement campaign

345 Ambient measurements of PM_{2.5} and 16 PAH species were collected from a dense network of measurement
sites in Hamilton, Ontario during June/July 2009 and December 2009. These measurements are described
in Anastasopoulos et al. (2012), where they found a high level of intra-urban variability for the PAHs;
3-4 times more variable than PM_{2.5} concentrations.

There were 43 measurement sites operating during the summer period (see Fig 4a), and 46 sites
350 during the winter period. All measurements are from 2-week integrated time frames (24 June to
8 July and 2 to 16 December) taken with URG personal pesticide samplers, which collected gas
and particle-phase PAHs less than 2.5 μm in diameter in 40 m³ of sample air. The PM_{2.5} measurements
were made at the same sites using a three-stage Harvard Cascade Impactor. The particle-phase
PAHs (up to 2.5 μm in diameter) were collected on a Teflon filter, gas-phase PAHs were collected
355 in polyurethane foam (PUF), and total (gas + particle) PAHs concentrations were reported in ng/m³
as determined by gas chromatography/mass selective detection. PM sample filter masses were determined
by gravimetric analysis. (Anastasopoulos et al., 2012)

O₃ measurements that were used to correct the Hamilton BaP measurements came from three
monitoring sites in the Hamilton region ("Downtown", "Mountain", and "West") from the Ontario
360 Ministry of Environment and Climate Change (MOECC) website for historical air quality data
(<http://www.airqualityontario.com/history/>).

3.2 National Air Pollution Surveillance Program

NAPS is a Canadian program to provide accurate and long-term air quality data of a uniform standard
across the country. NAPS is managed under a cooperative agreement between ECCC and the



365 provinces, territories, and some municipal governments. There are currently 286 NAPS measure-
ment sites in 203 communities located in every province and territory [www.ec.gc.ca/rnsps-naps/].

Under this program, PAH samples were collected over 24 hours, beginning and ending at midnight
(local), typically every 6 days, with a sample volume range of 600-800 m³ (Environment Canada,
2013). Benzene samples were collected in 6-L stainless steel canisters over 24 hours, starting at
370 midnight, every 3 days (Galarneau et al., 2016).

Within the Pan Am domain, total PAHs (gas+particle-phases combined) and benzene were measured
at eight NAPS sites (listed in Table A.1 in the supplemental material; Fig. 3), and their 2009
data were downloaded from the following url: <http://maps-cartes.ec.gc.ca/rnsps-naps/data.aspx>.

For BaP measurement corrections, the NAPS network also measures hourly O₃ at four of these
375 eight PAH/benzene sites (Windsor, Hamilton, Simcoe, and Egbert). Two of the missing sites (Toronto
and Etobicoke) had nearby O₃ measurements from MOECC, but the last two (Burnt Island, and
Point Petre), which are rural sites, had no O₃ measurements nearby. Therefore, BaP could only be
corrected at six of the eight NAPS sites in the Pan Am domain.

3.3 National Air Toxics Trends Stations network

380 NATTS is an a U.S. program to monitor toxic air pollutants in accordance with the U.S. Government
Performance Results Act, which requires the U.S. EPA to reduce the risk of cancer and other serious
health effects associated with hazardous air pollutants (HAPS) by achieving a 75% reduction in air
toxics emissions chemicals, based on 1993 levels (U.S. EPA, 2009). Regulated under the Clean Air
Act are 188 HAPS species including benzene and the seven PAHs in this study.

385 Every six days, 24-hour ambient air samples are collected starting at midnight LT. Analysis of the
samples is done by high resolution gas chromatography/mass spectrometry (GCMS) Selective Ion
Monitoring (SIM) mode to get total (gas + particle) PAH concentrations, and benzene concentrations
(Eastern Research Group, Inc., 2009).

There are 115 NATTS sites within the model domain (Table A.1 in the supplemental material,
390 Fig. 3), but only 21 sites measured PAHs, while 113 sites measured benzene. Those data were down-
loaded from the following url: www.epa.gov/ttnamti1/toxdat.html#data. Measurement methods in
NATTS are very similar to those of NAPS.

Since O₃ was not measured at the NATTS sites, NATTS BaP was corrected with the nearest O₃
monitor data found at the U.S. EPA and CASTNET websites: www.epa.gov/outdoor-air-quality-data/download-daily-data
395 and <https://java.epa.gov/castnet/reportPage.do>, respectively.

3.4 Integrated Atmospheric Deposition Network

IADN was mandated by the 1987 Canada-U.S. Water Quality Agreement, and was initiated in 1990
to measure atmospheric concentrations of persistent toxic pollutants in the Great Lakes basin. There
are nine IADN sites total within our Pan Am model domain, and they are listed in Table A.1 of the



400 supplemental material (see also Fig. 3). Six of the nine IADN sites report gas- and particle-phase
PAH atmospheric concentrations separately (labelled “PAHs” in Table A.1), and a different set of six
sites report wet deposition of PAHs (labelled “PAH wet dep” in Table A.1) using sampled precipi-
tation concentrations (Blanchard et al., 2005). Thus, these data can be used to evaluate the model’s
gas-particle partitioning and deposition, respectively. Benzene was not measured by IADN, nor was
405 C_{TSP} or PM_{10} in 2009, with the unfortunate result that K_p can not be calculated directly from the
IADN measurements. O_3 was also not measured by IADN, necessitating the use of the nearest O_3
monitors in order to carry out the BaP oxidation correction. This latter step was possible only for
observation stations at Cleveland and Chicago. The other four IADN air sites were rural/background
locations, and did not have any O_3 measurements nearby.

410 PAHs were collected by high-volume sampler for periods of 24 hours beginning at 08:00 Eastern
Standard Time, every 12 days. At Canadian IADN sites, glass fiber filters and PUF sorbent collected
the particulate and gaseous fractions, whereas the U.S. stations collected PAHs with quartz fiber
filters and XAD resin (Blanchard et al., 2005). Sample volume for the U.S. method is about 800 m^3 ,
but is 400 m^3 for the Canadian method to minimize breakthrough of volatile species during warm
415 summer months (Blanchard et al., 2005).

Wet deposition of PAHs are measured with MIC-B precipitation collectors. The U.S stations used
XAD-2 resin column cartridges for accumulating the organics on a 28-day cumulative basis, while
the Canadian stations use a dichloromethane solvent extraction system, also on a 28-day cumulative
basis. Both countries collect samples on a monthly basis. Note that one of the six wet deposition
420 sites, St Clair, Ontario (STC), only had valid measurements during February 2009, which was not a
time period simulated here. Therefore, only five IADN sites appear in our wet deposition analysis in
Section 4.4 below.

Note that Point Petre and Burnt Island are NAPS stations co-located with IADN. IADN data were
downloaded from the following url: <http://open.canada.ca/data/en/dataset/531d6054-4179-4883-8022-1175cdfb6911>.

425 4 Model Evaluation

In this section we evaluate GEM-MACH-PAH’s performance for benzene and PAH surface con-
centrations, their spatial variation, gas-particle partitioning, and wet deposition. We also assess the
sensitivity of the model output to PAH emission factors for mobile sources.

4.1 PAH concentrations in the Hamilton region

430 GEM-MACH-PAH output for gas + fine-PM PAH were compared to measurements of same from
the 2009 Hamilton campaign (Anastasopoulos et al., 2012). Fig 4a shows a map of measured and
modelled fluoranthene concentrations (14-day average) in the summer time period, as well as their
differences and ratios. Here we see that GEM-MACH-PAH has captured intra-city variability, and



that the differences between observations and simulated values are, at a maximum, $2.8\times$ too high.
435 The model is biased low in the upwind/background areas of the city, and a high in the eastern areas of
the city (Fig. 4a), and this pattern is seen across all seven PAHs. The spatial pattern in the PAH bias is
less apparent when PAH/PM_{2.5} ratios are plotted (in ng/μg – shown in Fig. E.1 in the supplemental
material) – removing the dependency on modelling PM correctly (since fractions of the PAH are
particulate). Therefore, the spatial pattern in the PAH bias is mainly due to the pattern in the model
440 PM bias, which is shown in Fig. E.2 in the supplemental material.

When the spatial variability is represented by the standard deviation over the mean (σ/mean), the
model achieves very similar spatial variability to the measurements (Fig. 4b). The scatter plot of
model vs measurements for summertime fluoranthene concentrations (Fig. 5a, FLRT selected as a
good example) has correlation coefficient R^2 of 0.57, and the slope of the best-fit line is very close
445 to 1. The other PAH species had similar results, where, except for FLRT, the slopes and R^2 values
were better in the winter than in the summer.

The model bias (given as a model/measurement ratio) for all PAHs is shown as box and whiskers
in Fig. 5b. Here we see that wintertime biases are smaller than those in the summertime for all PAHs
except for ANTH. The four lightest PAHs (left side of Fig. 5b) have model/measurement ratios near
450 1 (except summertime PHEN), but the three heaviest PAHs, are biased high (except for wintertime
CHRY). We will see this same pattern for the model bias (small for lighter PAHs, high for BaA and
BaP) in the next sections as well.

BaA and BaP are the most reactive of the heavier species, thus the lack of O₃ correction to the
BaA measurements may be partially responsible for the model-measurement differences. However,
455 mean O₃ for the three measurement stations in the Hamilton region was only 20-26 ppbv/day, thus
the O₃-corrected BaP was approximately 20% greater than the reported BaP concentrations. The
median BaP bias was brought down to 6.2 from 7.6 in the summer, and 5.5 from 6.3 in the winter
- these are shown as the purple boxes in Fig. 5b. Additional reactions with BaA and BaP, such as
with NO₃, are noted in the literature (Keyte et al., 2013; Mu et al., 2017), but were not included in
460 GEM-MACH-PAH at this time, given larger uncertainties in those reactions. However, our model
biases appear to indicate that those missing reactions may need to be considered for further model
improvement.

In order to remove the impact of the model's PM predictions on the PAH comparison, we also
plotted the PAH/PM_{2.5} model-over-measurement ratios (shown in Fig. E.3). There we see all of the
465 ratios reduced – which improves results for the heavier PAHs, but increases the low bias for the
lighter PAHs. The reason the bias decreases for all seven PAHs is that the model PM_{2.5} is overesti-
mated by a factor of 2 in the summertime, and a factor of 1.4 in the wintertime (average across all
sites in the Hamilton region).



4.2 PAH and benzene concentrations from the NAPS, NATTS, and IADN networks

470 Modelled 24-hour-average total (gas+particle) PAH and benzene concentrations can be evaluated
with every-6th-day measurements from the NATTS, NAPS, and IADN surface measurement net-
works, which sample much of the model domain well (Fig. 3). As with the Hamilton evaluation, the
model has very good agreement for seasonal averages at the monitoring network sites for benzene,
phenanthrene, anthracene, fluoranthene, and pyrene, which all have model/measurement ratios (red
475 and blue boxes) close to 1, and their concentrations (green and orange boxes) overlapping in Fig. 6a.
The 24-hour average model (daily) and measurements (every 6th day) have been averaged over each
of the 3-month time periods. BaA and CHRY are within a factor of 5 of the measurements in the
summertime, but worse in the wintertime. BaP is overestimated by the model in both summer and
winter by about a factor of 10, although the measurement-corrected BaP has a slightly reduced bias.
480 We have not shown the O₃-corrected BaP measurements in the plots because the changes are small,
similar to the Hamilton plot (Fig. 5a).

When the model biases are examined more closely we find a few patterns to determine the
cause(s). The following list summarizes some observations from our evaluation of each model-
measurement pair (24-hour averages, not seasonal averages):

485 – **By site - overestimations:** all PAHs are significantly overestimated at the Kennedy Township,
Pennsylvania (NW of Pittsburgh) NATTS site (Fig 6b). There appears to be a major emissions
point source near that station that is emitting too much PAH in our model compared to reality.
There are in fact hundreds of point sources in the emissions inventory that are within 20 km
of Kennedy Township, but one in particular emits a relatively large amount of VOCs, and is
490 associated with the “Secondary Metal Production; Aluminum; Raw Material Charging” source
category, which has very large PAH-to-TOG EFs in Galarneau et al. (2007) because aluminum
smelter emissions are largely particulate, so expressing EFs as a large fraction of TOG was
somewhat artificial. However, our results indicate that the PAH EFs for that PAH speciation
profile (1036b) should be reduced substantially compared to Galarneau et al. (2007). In order
495 to ensure that this facility did not begin operation *after* 2009 - which is a risk when using a
2011 inventory to model the year 2009 and would result in a large overestimation as well, we
have further verified that the facility existed and was emitting similar VOC amounts in the
NEI2008 inventory as well.

PHEN (Fig. 7c) and ANTH (not shown) are also greatly overestimated in New York City,
500 however, none of the other PAHs are biased particularly high there. However, we note that
the measurements for New York City appear erroneously low, as the reported PHEN concen-
trations there are around the same magnitude as those in Underhill, VT (Fig. 7c), which is a
background site, near a national park.



505 Most PAHs are also overestimated at the Gary, Indiana site (Fig 6b)), which may also have a nearby major point emissions source that is too high compared to reality. The heavier PAHs (BaA, CHRY, and BaP) are also overestimated at the Toronto Gage Institute NAPS site, but are only slightly higher there than the average model/measurement ratio for those species (not shown).

– **By site - underestimates:** all PAHs are markedly underestimated at the Liberty, Pennsylvania site (e.g., Figs. 6b, and 7c), implying that there may be industry emissions of PAHs here that are missing, mis-allocated, or misplaced in the NEI2011 inventory, or an improper PAH speciation profile applied. Similarly, PAHs are underestimated in Buffalo, New York and at Franklin Furnace, Ohio. As these are not large cities, there may be industrial emissions that are not reported in the NEI2011 emissions inventory (or are reported at too low levels) -
515 perhaps because those facilities shut down in 2010 (or installed emission control technology), which would mean the problem simply lies in using a 2011 inventory to model 2009.

However, when we further investigated stacks near Buffalo, NY, we found that the facility with the largest CO and VOC emissions had zero PAH emissions. This facility is associated with the generic process of “Primary metal production; By-product Coke Manufacturing”, which did not have an associated PAH-to-TOG profile in Galarneau et al. (2007), because the source category codes that follow it (such as flushing liquor circulation tank, excess-ammonia liquor tank, tar dehydrator, tar interceding sump, tar storage, etc) are not expected to emit PAHs to air. However, our results imply that the PAH speciation profile for “By Product Coke Oven Stack Gas” (0011b) would have been more appropriate for this facility and its use might eliminate
525 the model bias near Buffalo in future studies.

– **By month:** All PAH species have lower mod/meas ratios in the summer than in the winter (shown in Fig. 6a by season for all PAHs and in Fig. 6c for FLRT by month) – implying that modelled hydroxyl radical (OH) and/or PM biases (which have strong seasonal cycles) are impacting modelled PAHs. For example, if model OH is too high in the summer, or too low in the winter, this would cause the U-shaped pattern that we see when plotting model/measurement ratio vs. month (Fig. 6c) and it would be particularly pronounced for the lighter, gas-phase PAHs, which it is. Another possibility is seasonal bias in the representation of atmospheric vertical stability: if the modeled stability is too low in the summer and too high in the winter, then winter emissions will tend to be trapped in inversions more than observed, and summer emissions will be diluted by excessive vertical mixing. However, evidence in Makar et al. (2010) and Stroud et al. (2012) suggest that model stability is too high (not too low) for the
535 summer time period in those studies.

– **By season:** For the four lightest PAHs, the model/measurement ratios are <1 in the summer, and >1 in the winter (Fig. 6a). As mentioned above, this is likely due to modelled OH being



540 too high in the summer and too low in the winter. BaA and CHRY follow a similar seasonal difference but do not straddle the ratio=1 mark.

BaP, on the other hand has a model/measurement ratio that is slightly higher in the summer than in the winter (Fig. 6a). For BaP, the OH bias could be offset by an opposite O₃ bias in the model. Indeed, it has been shown (Makar et al., 2010; Stroud et al., 2012) that the processes
545 in GEM-MACH cause urban, surface O₃ to be too low in the summertime, due to insufficient vertical mixing and excessive titration from NO_x, and surface PM tends to be too high in the wintertime due to overestimation of wintertime atmospheric stability (e.g., lack of an urban heat island parameterization in the driving meteorology). These factors, together with the BaP measurement bias due to on-filter reaction with O₃, may explain the high model BaP bias.

550 Thus, the generally high bias of modelled BaP may be due to additive OH, O₃ and PM model biases (plus the missing O₃ denuder technology in the measurements), impacting BaP more than the other species because BaP has the highest O₃ reactivity, and the highest particulate fraction of the seven PAHs examined here.

When the five measurement sites mentioned in "By Site", above (Kennedy Township, PA; Gary, IN; Liberty PA; Buffalo, NY; Franklin Furnace, OH) are removed from the NATTS analysis (because
555 errors in their nearby emissions were identified), model-measurement correlation (R) and slopes improve. For example, the model vs. measurement best-fit-line slope for PHEN doubles from 0.3 to 0.6 when those sites are removed, and its R increases from 0.16 to 0.32. The slopes and R values of the four heaviest PAHs all move from *negative* to positive. PYR has the largest improvement,
560 going from slope=-0.049 and R=-0.028 to slope=0.26 and R=0.35. To the extent that the model prediction errors at the other sites may reflect emissions inaccuracy, having an accurate major point emission inventory for the time period modelled, along with proper PAH speciation profiles are extremely important requirements for modelling PAHs well at high resolution. The cases with large discrepancies mentioned above highlight the need to be as specific as possible when assigning source
565 category codes to facility processes (which is difficult given that there are tens of thousands of point sources in the inventories).

That said, when using a paired t-test on all data to examine whether the summertime and wintertime modelled averages are the same as the measured averages, we found that the model was indistinguishable from the measurements for all PAH species (t<1 and p>0.05), *except* for wintertime BaP (which has t>1, and p<0.05, however, even with the O₃-corrected measurements). At
570 finer time scales (e.g., *daily* model-measurement pairs) only modelled ANTH was statistically indistinguishable from measurements. Therefore, GEM-MACH-PAH can accurately model benzene and PAHs seasonally, but not daily.



4.2.1 Sensitivity of model to mobile emission factors

575 As discussed in the previous section, ensuring the accuracy of major point source emissions is important for model-measurement agreement near industrial locations. However, those major point source emissions tend to be located far from large population centres where human exposure is concentrated. In our inventory, mobile emissions make up 44%, 45%, 19%, 32%, 14%, 21%, and 30% of total PAH emissions, for PHEN, ANTH, FLRT, PYR, BaA, CHRY, and BaP, respectively, in our continental model domain, and studies have shown that the bulk of emissions within population centers is likely to originate from on-road mobile sector emissions (Dunbar et al., 2001; Pachón et al., 2013; Kuoppamäki et al., 2014; Miao et al., 2015). Thus, in order to accurately model ambient PAHs in urban centres, the uncertainty in emission factors from on-road vehicles may play a more significant role than major point sources.

585 We have thus carried out 2-week sensitivity simulations (9-24 May and 18 Oct-2 Nov 2009) wherein the mobile emissions of PAHs were scaled by factors of 0.5 and 1.5. This is approximately equivalent to the 25th and 75th percentiles in the range of emission factors found in the recent literature.

In Fig. 7, we show the surface PHEN time series from the measurements, base model run, and 0.5 and 1.5 scaled model runs at the IADN, NAPS, and NATTS sites. It is clear that – while a relatively small PAH source overall – changes to mobile emissions makes a large change in ambient PAH concentrations at certain urban locations, such as Philadelphia, PA, New York, NY, and Burlington, Etobicoke, and Windsor, ON.

On average, there is about a 20-30% increase in PAH concentrations when mobile emissions are increased by 50%, and a 5-10% decrease in PAH concentrations when mobile emissions are decreased by 50% (Fig. 8, PHEN and BaP shown as examples) – with a larger sensitivity in the summer than the winter, and slightly larger sensitivity at NATTS (U.S.) sites than at NAPS (Canada) sites. The predicted ambient concentrations generally follow the increase or decrease in on-road mobile emissions monotonically.

600 4.3 Gas-particle partitioning of PAHs

The IADN network also allows us to assess model predictions of gas-particle partitioning of PAHs at six sites (24-hour averages, every six days). Fig. 9 shows a time series of pyrene particulate fraction (ϕ_k). Both model and measurements show higher ϕ_k in the wintertime, when there are higher PM concentrations for PAH adsorption, and lower temperatures. Generally, the model seems to underestimate ϕ_k at background sites (e.g., Burnt Island), and overestimate ϕ_k at urban sites (e.g, Chicago), and this is true for all PAH species. Thus, in Fig. 10, which shows the results for all PAHs at all sites, the model (green) has a larger range of ϕ_k than the measurements (orange). This is caused by the model over- and underestimating PM concentrations at urban and rural sites,



respectively. For example, wind-blown dust is not included in the model; however, it is known to
610 be a potentially significant contributor to total PM in rural areas. Also, due to an underestimate of
vertical mixing in the model, PM tends to be biased high in urban areas, near emissions, due to a
lack of a parameterization for urban heat islands (Stroud et al., 2012).

Comparing Fig. 10 (blue boxes) to Fig. 2b (green boxes), we see significant improvement over
the original AURAMS-PAH partitioning due to the improved K_{SW} parameters described in Section
615 2.2.1.

Generally, the gas-particle partitioning scheme in the model results in model/measurement ratios
well within an order of magnitude, given by the gray lines in Fig. 10. ϕ_k for BaA and CHRY are
still underestimated, but this may be related to modelled PM errors as noted earlier. We note that
the addition of C_{TSP} or even PM_{10} measurements at IADN sites (which existed in 2002, but not in
620 2009) would allow for the calculation of measured partitioning coefficients ($\log K_p$, Eq. (2)), which
could be used to validate the modelled $\log K_p$ in future work. Since K_p takes total suspended particle
into account, it removes the dependency on modelled PM, thus would increase confidence that the
modelled partitioning is working properly, despite model errors in PM.

The fact that the GEM-MACH-PAH model partitioning of BaA and CHRY (and BaP to a lesser
625 extent) puts too much concentration in the gas phase, may help explain why these species in particu-
lar are overestimated in the model. While in the gas phase, these species are less likely to be removed
from the atmosphere, so their concentrations would erroneously build up in the model.

4.4 Wet deposition of PAHs

When compared to the IADN one-month wet deposition measurements, the model generally over-
630 estimates wet deposition for all PAHs, as is shown in Table 2, and Fig. 11. In Fig. 11, the blue
lines shows the ideal 1:1 model:measurement ratio, and most of the data lie well above these lines.
By site (Fig. 11a), the modelled wet deposition was slightly better at urban locations (Toronto and
Cleveland) than suburban and background sites (Burlington, Sturgeon Point, and Point Petre). By
month (Fig. 11b), the wet deposition from the model is best represented in June and July, whereas,
635 wet deposition is greatly overestimated in the winter, implying that the current snow adsorption
parameterization may be too effective at removing PAHs in the model.

The IADN measurements, which report the concentration of PAHs in the collected rainwater (in
pg/L), were converted to pgPAH/m^2 in order to compare to the wet deposition output of the model.
However, this conversion assumes that the volume of rainwater reported by IADN was the *total* rain
640 fall in the container's cross-sectional area, and in fact, it is not. The IADN wet deposition collectors
are actually known to *not* sample all of the rainfall because the samplers aren't in the correct configu-
ration to get an accurate rainfall measurement (Dryfhout-Clark, personal communication). When we
compared the actual rainfall amounts (from separate meteorological rain gauge data) to IADN rain
volumes at the Point Petre location in January 2009, we found that only 68% of the total rainfall was



645 captured by the wet deposition sampler. Therefore, if that correction factor were applied to all IADN
wet deposition measurements, they would increase by a factor of approximately 1.5, which would
improve our comparison, but not eliminate the total bias. If IADN sites added separate, accurate rain
gages, then we could apply a “rainfall correction” to the IADN wet deposition measurements in a
thorough, consistent way in future work.

650 Aside from the measurement bias, the modelled PAH wet deposition bias will also be dependent
on the model’s overall ability to predict accurate rainfall. We compared the modelled daily accumu-
lated precipitation to the precipitation measured with the accurate gages at Burnt Island and Point
Petre, and found that, while the model’s median precipitation bias was only about 0.2 mm, there was
a large standard deviation, and there were some incidences where the model greatly over-predicted
655 high rain events. Those incidences would result in greater modelled wet deposition of PAHs than was
measured, and because we sum over a month, there is a significant likelihood of an overprediction
occurring in that long time frame. Indeed, the median ratios in Table 2, which are less sensitive to
high outliers than the mean is, are substantially lower than the mean for most species.

Therefore, the model bias in wet deposition would appear to be caused by three additive factors:
660 (1) measurements themselves having a negative bias relative to reality, due to insufficient capture of
the net fluxes of precipitation, (2) modelled precipitation being biased high, and (3) a positive model
bias in atmospheric PAH concentrations (which was highest for BaA and BaP in particular).

The reverse reasoning can be applied, whereby we can see if high atmospheric concentrations of
BaA and BaP were caused by too little wet deposition. In this case, since both of these species have
665 correspondingly high wet deposition in the model (Fig. 11), it would appear that underestimation of
wet deposition is probably not one of the causes.

Fig. 12 shows results from a sample month (June 2009) for pyrene (PYR). The spatial distribution
of wet deposition was not captured, with the model predicting lower PYR deposition in Toronto and
Sturgeon Point than the measurements, higher at Point Petre, and about equal at Burlington. This
670 spatial pattern is *not* the same for all PAHs, and even differs by month for the same PAH (e.g., PYR
deposition in the next month, July, is low at Point Petre, high at Toronto, and highest in Burlington).
Given that wet deposition of PAHs relies on getting many model factors correct (meteorology, scav-
enging parameters, atmospheric concentrations, etc), it not surprising that the model error for PAH
wet deposition is large, but it is at least promising to see that there are no particular sites where the
675 model is consistently too high or too low, rather the errors in spatial distribution are haphazard and
may be due to propagation of error, rather than any major error with the PAH scavenging scheme
itself.



5 Conclusions

Through this work, a high resolution chemical transport model for North American air toxics was
680 created that allows us to see variations within a densely populated area. GEM-MACH-PAH was de-
veloped and run at 2.5-km resolution for air quality forecasting and for simulating the impacts of
emissions scenarios. Relative to AURAMS-PAH, on-road mobile emissions, gas-particle partition-
ing, and scavenging were all improved in this study. Mobile PAH emission factors from different
sources were evaluated and the MOVES 2014 factors achieved the best model results compared to
685 those in the recent literature and in the SPECIATE database. Parameters used in the gas-particle
partitioning scheme (particularly $K_{SW,k}$) were improved based on the observed relationship be-
tween $\log K_p$ and $\log p$, resulting in much better agreement between model and observations than
was achieved with AURAMS-PAH. This is an important improvement because the particle/gas par-
titioning determines deposition and inhalation - both pathways of exposure in humans and ecosys-
690 tems. Finally, we added snow scavenging, which was not a process included in AURAMS-PAH, and
updated wet scavenging parameters.

Overall, GEM-MACH-PAH simulates benzene and six semi-volatile PAHs (PHEN, ANTH, FLRT,
PYR, BaA, CHRY) at seasonal time-scales with concentrations statistically indistinguishable from
observations, at 2.5-km resolution. For the seventh PAH species, BaP; its summertime average is
695 simulated to a similar level of accuracy. However, it appears the model's OH, O₃, and PM biases
were additive, resulting in a wintertime average that is biased significantly high for BaP. Lack of re-
moval of BaP via wet deposition was ruled out as a cause, but the lack of an O₃ denuder system in the
measurements contributes a small amount to the model-measurement differences as well. When we
corrected BaP measurements using the Schauer et al. (2003) O₃ relationship, we found reductions
700 of about 20% in the model/measurement ratios, improving the model performance.

Our results have shown that the major point source emissions play a large role in producing ac-
curate model results near industrial facilities, but also that the uncertainty associated with on-road
mobile emission factors plays a large role in the accuracy of simulations near and within cities. In
fact, we have determined from our sensitivity test that the GEM-MACH-PAH model has a linear re-
705 sponse to a 50% variation in mobile emission factors, simulating concentrations that vary up to 30%.
The spatial variability at high resolution is modelled to within 50% of Hamilton, Ontario mea-
surements, although the model places higher concentrations in polluted areas, and lower concentrations
in background areas than the measurements suggest, which is correlated to the spatial distribution
of the model's PM bias. With this information, we can use the high-resolution GEM-MACH-PAH
710 model for studying vehicle emissions scenarios in order to determine intra- and inter-city variations
due to motor vehicles, with an understanding of the range of uncertainty that such a study would
have.

Additional improvements to PAH modelling efforts could be achieved with general model im-
provements to its treatment of particulate matter (e.g., better parameterizations for wind-blown dust



715 in rural areas, and better parameterizations for urban heat islands in urban areas). Also, additional
reactions with particulate BaA and BaP in the model (e.g., with NO_3) may reduce their bias further.
It would also be beneficial to any future model/measurement studies, if the PAH measurement net-
works utilized ozone denuder technology so that particle-phase PAHs are not underestimated in the
reported observations, as well as improved and consistent rain collection at wet deposition measure-
720 ment sites. Partitioning could be better assessed if sites that measure PAH gas and particle phases
separately (like IADN in this study) also measured C_{TSP} or PM_{10} .

6 Data and code availability

Data availability: Please refer to Section 3 for the websites where the observations can be freely
downloaded.

725 Model code availability: GEM-MACH - Atmospheric chemistry library for the GEM numerical at-
mospheric model Copyright (C) 2007-2013 - Air Quality Research Division and National Prediction
Operations division, Environment and Climate Change Canada. This library is free software which
can be redistributed and/or modified under the terms of the GNU Lesser General Public License as
published by the Free Software Foundation; either version 2.1 of the License, or any later version.

730 The CHEM code can be downloaded from this Zenodo site: <https://zenodo.org/record/1162252#.Wm9DtK1IJZQ>,
DOI:10.5281/zenodo.1162252.

Acknowledgements. The authors gratefully acknowledge funding from ECCC's Climate Change and Air Pollu-
tion program (CCAP, formerly called the Clean Air Regulatory Agenda). Thank you to Angelos Anastasopoulos
and Amanda Wheeler for the Hamilton measurement data, to Helena Dryfhout-Clark for consultation on IADN
735 data products, and Armaan Ladak for his help with the measurement data. Figures were made using the R-based
OpenAir package (Carslaw and Ropkins, 2012; Carslaw, 2015).



References

- Agrawal, H., Welch, W. A., Miller, J. W., and Cocker, D. R.: Emissions Measurements from a Crude Oil Tanker at Sea, *Environ. Sci. Technol.*, 42, 7098–7103, doi:10.1021/es703102y, 2008.
- 740 Anastasopoulos, A. T., Wheeler, A. J., Karman, D., and Kulka, R. H.: Intraurban concentrations, spatial variability, and correlation of ambient polycyclic aromatic hydrocarbons (PAH) and PM_{2.5}, *Atmospheric Environment*, 59, 272–283, doi:10.1016/j.atmosenv.2012.05.004, 2012.
- Aulinger, A., Matthias, V., and Quante, M.: Introducing a partitioning mechanism for PAHs into the Community Multiscale Air Quality modeling system and its application to simulating the transport of benzo(a)pyrene over Europe, *J. App. Met. and Clim.*, 46, 1718–1730, doi:10.1175/2007JAMC1395.1, 2007.
- 745 Baklanov, A., Schlünzen, K., Suppan, P., Baldasano, J., Brunner, D., Aksoyoglu, S., Carmichael, G., Douros, J., Flemming, J., Forkel, R., Galmarini, S., Gauss, M., Grell, G., Hirtl, M., Joffre, S., Jorba, O., Kaas, E., Kaasik, M., Kallos, G., Kong, X., Korsholm, U., Kurganskiy, A., Kushta, J., Lohmann, U., Mahura, A., Manders-Groot, A., Maurizi, A., Moussiopoulos, N., Rao, S. T., Savage, N., Seigneur, C., Sokhi, R. S., Solazzo, E., Solomos, S., Sørensen, B., Tsegas, G., Vignati, E., Vogel, B., and Zhang, Y.: Online coupled regional meteorology chemistry models in Europe: current status and prospects, *Atmos. Chem. Phys.*, 14, 317–398, doi:10.5194/acp-14-317-2014, 2014.
- Bidleman, T.: Atmospheric processes: wet and dry deposition of organic compounds are controlled by their vapor-particle partitioning, *Environ. Sci. Technol.*, 22, 361–367, 1988.
- 755 Bidleman, T. F. and Foreman, W. T.: Vapor-particle partitioning of semivolatile organic compounds, in: *Sources and Fates of Aquatic Pollutants*, pp. 27–56, American Chemical Society, 1987.
- Blanchard, P., Audette, C. V., Hulting, M. L., Basu, I., Brice, K. A., Backus, S. M., Dryfhout-Clark, H., Froude, F., Hites, R. A., Neilson, M., and Wu, R.: Atmospheric deposition of toxic substances to the Great Lakes: IADN results through 2005, Report, Air Quality Research Division, Environment Canada; Great Lakes National Program Office, U.S. EPA, 4905 Dufferin St., Toronto, ON, M3H 5T4, Canada; 77 West Jackson Blvd, Chicago, IL, 60604, USA, 2005.
- 760 Brubaker, W. W. and Hites, R. A.: OH reaction kinetics of polycyclic aromatic hydrocarbons and polychlorinated dibenzo-p-dioxins and dibenzofurans, *J. Phys. Chem.*, 102, 915–921, 1998.
- Bucheli, T. D. and Gustafsson, O.: Quantification of the soot-water distribution coefficient of PAHs provides mechanistic basis for enhanced sorption observations, *Environ. Sci. Tech.*, 34, 5144–5151, doi:10.1021/es000092s, 2000.
- Carslaw, D. C.: The openair manual: open-source tools for analysing air pollution data, Technical report, <http://www.openair-project.org>, 2015.
- Carslaw, D. C. and Ropkins, K.: Openair: an R package for air quality data analysis, *Environ. Modell. Software*, 77, 52–61, doi:10.1016/j.envsoft.2011.09.008, 2012.
- 770 Chen, Y.-C., Lee, W.-J., Uang, S.-N., Lee, S.-H., and Tsai, P.-J.: Characteristics of polycyclic aromatic hydrocarbons (PAH) emissions from a UH-1H helicopter engine and its impact on the ambient environment, *Atmospheric Environment*, 40, 7589–7597, doi:10.1016/j.atmosenv.2006.06.054, 2006.
- Côté, J., Desmarais, J.-G., Gravel, S., Méthot, A., Patoine, A., Roch, M., and Staniforth, A.: The Operational CMC–MRB Global Environmental Multiscale (GEM) Model. Part II: Results, *Monthly Weather Review*, 126, 1397–1418, doi:10.1175/1520-0493(1998)126<1397:TOCMGE>2.0.CO;2, 1998a.



- Côté, J., Gravel, S., Méthot, A., Patoine, A., Roch, M., and Staniforth, A.: The Operational CMC–MRB Global Environmental Multiscale (GEM) Model. Part I: Design Considerations and Formulation, *Monthly Weather Review*, 126, 1373–1395, doi:10.1175/1520-0493(1998)126<1373:TOCMGE>2.0.CO;2, 1998b.
- 780 Dachs, J. and Eisenreich, S. J.: Adsorption onto aerosol soot carbon dominates gas-particle partitioning of polycyclic aromatic hydrocarbons, *Environ. Sci. Technol.*, 34, 3690–3697, doi:10.1021/es991201, 2000.
- Daly, G. L. and Wania, F.: Simulating the influence of snow on the fate of organic compounds, *Environ. Sci. Technol.*, 38, 4176–4186, doi:10.1021/es035105r, 2004.
- Dharmapala, R., Claiborn, C., Jimenez, J., Corkill, J., Gullett, B., Simpson, C., and Paulsen, M.:
785 Emission factors of PAHs, methoxyphenols, levoglucosan, elemental carbon and organic carbon from simulated wheat and Kentucky bluegrass stubble burns, *Atmospheric Environment*, 41, 2660–2669, doi:10.1016/j.atmosenv.2006.11.023, 2007.
- Domine, F., Taillandier, A.-S., and Simpson, W. R.: A parameterization of the specific surface area of seasonal snow for field use and for models of snowpack evolution, *J. Geophys. Res.*, 112, doi:10.1029/2006JF000512,
790 2007.
- Dunbar, J. C., Lin, C. I., Vergucht, I., Wong, J., and Duran, J. L.: Estimating the contributions of mobile sources of PAH to urban air using real-time PAH monitoring, *Sci. Tot. Environ.*, 279, 1–19, doi:10.1016/S0048-9697(01)00686-6, 2001.
- Eastern Research Group, Inc.: Technical Assistance document for the National Air Toxics Trends Stations
795 Program – Revision 2, Report, Office of Air Quality Planning and Standards, U.S. EPA, 601 Keystone Park Drive, Suite 700, Morrisville, NC 27560, 2009.
- Emmons, L., Walters, S., Hess, P., Lamarque, J.-F., Pfister, G., Fillmore, D., Granier, C., Guenther, A., Kinnison, D., Laepple, T., Orlando, J., Tie, X., Tyndall, G., Wiedinmyer, C., Baughcum, S., and Kloster, S.: Description and evaluation of the Model for Ozone and Related chemical Tracers, version 4 (MOZART-4), *Geosci. Model Dev.*, 3, 43–67, doi:10.5194/gmd-3-43-2010, 2010.
- 800 Environment Canada: 10 years of data from the National Air Pollution Surveillance (NAPS) network: DATA SUMMARY FROM 1999 to 2008, Report, Analysis and Air Quality Section, Air Quality Research Division, Science and Technology Branch, Toronto, ON, Canada, 2013.
- Franz, T. P. and Eisenreich, S. J.: Snow scavenging of polychlorinated biphenyls and polycyclic aromatic hydrocarbons in Minnesota, *Environ. Sci. Tech.*, 32, 1771–1778, doi:10.1021/es970601z, 1998.
- 805 Friedman, C. L. and Selin, N. E.: Long-range atmospheric transport of polycyclic aromatic hydrocarbons: a global 3-D model analysis including evaluation of Arctic sources, *Environ. Sci. Tech.*, 46, 9501–9510, doi:10.1021/es301904d, 2012.
- Galarneau, E., Makar, P. A., Sassi, M., and Diamond, M. L.: Estimation of Atmospheric Emissions of Six
810 Semivolatile Polycyclic Aromatic Hydrocarbons in Southern Canada and the United States by Use of an Emissions Processing System, *Environ. Sci. Technol.*, 41, 4205–4213, doi:10.1021/es062303k, 2007.
- Galarneau, E., Makar, P. A., Zheng, Q., Narayan, J., Zhang, J., Moran, M. D., Bari, M. A., Pathela, S., Chen, A., and Chlumsky, R.: PAH concentrations simulated with the AURAMS-PAH chemical transport model over Canada and the USA, *Atmos. Chem. Phys.*, 14, 4065–4077, doi:10.5194/acp-14-4065-2014, 2014.
- 815 Galarneau, E., Wang, D., Dabek-Zlotorzynska, E., Siu, M., Celso, V., Tardif, M., Harnish, D., and Jiang, Y.: Air toxics in Canada measured by the National Air Pollution Surveillance (NAPS) Program and their rela-



- tion to ambient air quality guidelines, *Journal of the Air & Waste Management Association*, 66, 184–200, doi:10.1080/10962247.2015.1096863, 2016.
- 820 Gariazzo, C., Silibello, C., Finardi, S., Radice, P., Pieranti, A., Calori, G., Cecinato, A., Perrino, C., Nussio, F., Cagnoli, M., Pelliccioni, A., Gobbi, G. P., and Filippo, P. D.: A gas/aerosol air pollutants study over the urban area of Rome using a comprehensive chemical transport model, *Atmos. Environ.*, 41, 7286–7303, doi:10.1016/j.atmosenv.2007.05.018, 2007.
- 825 Gong, W., Dastoor, A., Bouchet, V., Gong, S., Makar, P., Moran, M., Pabla, B., Ménard, S., Crevier, L.-P., Cousineau, S., and Venkatesh, S.: Cloud processing of gases and aerosols in a regional air quality model (AURAMS), *Atmos. Res.*, 82, 248–275, 2006.
- Gong, W., Makar, P. A., Zhang, J., Milbrandt, J., Gravel, S., Hayden, K. L., Macdonald, A. M., and Leaitch, W. R.: Modelling aerosol cloud meteorology interaction: A case study with a fully coupled air quality model GEM-MACH, *Atmos. Environ.*, 115, 695–715, doi:10.1016/j.atmosenv.2015.05.062, 2015.
- 830 Goriaux, M., Jourdain, B., Temime, B., Besombes, J.-L., Marchand, N., Albinet, A., Leoz-Garziandia, E., and Wortham, H.: Field comparison of particulate PAH measurements using a low-flow denuder device and conventional sampling systems, *Environ. Sci. Technol.*, 40, 6398–6404, doi:10.1021/es060544m, 2006.
- Hachikubo, A., Yamaguchi, S., Arakawa, H., Tanikawa, T., Hori, M., Sugiura, K., Matoba, S., Niwano, M., Kuchiki, K., and Aoki, T.: Effects of temperature and grain type on time variation of snow specific surface area, *Bull. Glac. Res.*, 32, 47–53, doi:10.5331/bgr.32.47, 2014.
- 835 Hall, D., Wu, C.-Y., Hsu, Y.-M., Stormer, J., Engling, G., Capeto, K., Wang, J., Brown, S., Li, H.-W., and Yu, K.-M.: PAHs, cabonyls, VOCs and PM_{2.5} emission factors for pre-harvest burning of Florida sugarcane, *Atmospheric Environment*, 55, 164–172, doi:10.1016/j.atmosenv.2012.03.034, 2012.
- Hanot, L. and Dominé, F.: Evolution of the surface area of a snow layer, *Environ. Sci. Technol.*, 33, 4250–4255, doi:10.1021/es9811288, 1999.
- 840 Hoff, J. T., Gregor, D., Mackay, D., Wania, F., and Jia, C. Q.: Measurement of the specific surface area of snow with the nitrogen adsorption technique, *Environ. Sci. Technol.*, 32, 58–62, doi:10.1021/es970225i, 1998.
- Jariyasopit, N., Zimmermann, K., Schrlau, J., Arey, J., Atkinson, R., Yu, T.-W., Dashwood, R. H., Tao, S., and Simonisch, S. L. M.: Heterogeneous reaction of particulate matter-bound PAHs and NPAHs with NO₃/N₂O₅, OH radicals and O₃ under simulated long-range atmospheric transport conditions: reactivity and mutagenicity, *Environ. Sci. Tech.*, 48, 10 155–10 164, doi:10.1021/es5015407, 2014.
- 845 Joe, P., Belair, S., Bernier, N. B., Bouchet, V., Brook, J. R., Brunet, D., Burrows, W., Charland, J. P., Dehghan, A., Driedger, N., Duhaime, C., Evans, G., Filion, A.-B., Frenette, R., de Granpré, J., Guiltepe, I., Henderson, D., Herdt, A., Hilker, N., Huang, L., Hung, E., Isaac, G., Jeong, C.-H., Johnston, D., Klaassen, J., Leroyer, S., Lin, H., MacDonald, M., MacPhee, J., Mariani, Z., Munoz, T., Reid, J., Robichaud, A., Rochon, Y., Shairsingh, K., Sills, D., Spacek, L., Stroud, C., Su, Y., Taylor, N., Vanos, J., Voogt, J., Wang, J. M., Wiechers, T., Wren, S., Yang, H., and Yip, T.: The Environment Canada Pan and ParaPan American Science Showcase Project, *Bulletin of the American Meteorological Society*, doi:10.1175/BAMS-D-16-0162.1, 2017.
- 850 Jonker, M. T. O. and Koelmans, A. A.: Sorption of polycyclic aromatic hydrocarbons and polychlorinated biphenyls to soot and soot-like materials in the aqueous environment: mechanistic considerations, *Environ. Sci. Technol.*, 36, 3725–3734, doi:10.1021/es020019x, 2002.



- Junge, C. E.: Basic considerations about trace constituents in the atmosphere as related to the fate of global pollutants, in: *Fate of pollutants in the air and water environments*, edited by Suffet, I. H., pp. 7–25, Wiley, New York, 1977.
- Kahan, T. F., Kwamena, N.-O., and Donaldson, D. J.: Heterogeneous ozonation kinetics of polycyclic aromatic hydrocarbons on organic films, *Atmos. Environ.*, 40, 3448–3459, 2006.
- 860 Keyte, I. J., Harrison, R. M., and Lammel, G.: Chemical reactivity and long-range transport potential of polycyclic aromatic hydrocarbons - a review, *Chem. Soc. Rev.*, 42, 9333–9392, doi:10.1039/c3cs60147a, 2013.
- Khalek, I. A., Bougher, T. L., and Merritt, P. M.: Phase 1 of the advanced collaborative emissions study, Report, Coordinating Research Council, INC., Mansell Rd, Alpharetta, GA, USA, 30022, 2009.
- 865 Kim, K., Jahan, S., Kabir, E., and Brown, R. J.: A review of airborne polycyclic aromatic hydrocarbons (PAHs) and their human health effects, *Environ. Int.*, 60, 71–80, doi:10.1016/j.envint.2013.07.019, 2013.
- Kuoppamäki, K., Setälä, H., Rantalainen, A.-L., and Kotze, D. J.: Urban snow indicates pollution originating from road traffic, *Environ. Poll.*, 195, 56–63, doi:10.1016/j.envpol.2014.08.019, 2014.
- Kwamena, N.-O., Thornton, J. A., and Abbatt, J. P. D.: Kinetics of surface-bound benzo(a)pyrene and ozone on solid organic and salt aerosols, *J. Phys. Chem.*, 108, 11 626–11 634, doi:10.1021/jp046161x, 2004.
- 870 Kwamena, N.-O. A., Staikova, M. G., Donaldson, D. J., George, I. J., and Abbatt, J. P. D.: Role of the Aerosol Substrate in the Heterogeneous Ozonation Reactions of Surface-Bound PAHs, *J. Phys. Chem.*, 111, 11 050–11 058, doi:10.1021/jp075300i, 2007.
- Lei, Y. D. and Wania, F.: Is rain or snow a more efficient scavenger of organic chemicals?, *Atmos. Environ.*, 38, 3557–3571, doi:10.1016/j.atmosenv.2004.03.039, 2004.
- 875 Liu, K., Duan, F., He, K., Ma, Y., and Cheng, Y.: Investigation on sampling artefacts of particle associated PAHs using ozone denuder systems, *Front. Environ. Sci. Eng.*, 8, 284–292, doi:10.1007/s11783-013-0555-7, 2014.
- Lohmann, R. and Lammel, G.: Adsorptive and Absorptive Contributions to the Gas-Particle Partitioning of Polycyclic Aromatic Hydrocarbons: State of Knowledge and Recommended Parametrization for Modeling, *Environ. Sci. Technol.*, 38, 3793–3803, doi:10.1021/es035337q, 2004.
- 880 Ma, Y.-G., Lei, Y. D., Xiao, H., Wania, F., and Wang, W.-H.: Critical review and recommended values for the physical-chemical property data of 15 polycyclic aromatic hydrocarbons at 25°C, *J. Chem. Eng. Data*, 55, 819–825, doi:10.1021/je900477x, 2010.
- Makar, P., Gong, W., Hogrefe, C., Zhang, Y., Curci, G., Zabkar, R., Milbrandt, J., Im, U., Balzarini, A., Baró, R., Bianconi, R., Cheung, P., Forkel, R., Gravel, S., Hirtl, M., Honzak, L., Hou, A., Jiménez-Guerrero, P., Langer, M., Moran, M., Pabla, B., Pérez, J., Pirovano, G., José, R. S., Tuccella, P., Werhahn, J., Zhang, J., and Galmarini, S.: Feedbacks between air pollution and weather, part 2: Effects on chemistry, *Atmos. Environ.*, 115, 499–526, doi:10.1016/j.atmosenv.2014.10.021, 2015a.
- 885 Makar, P., Akingunola, A., Aherne, J., Cole, A., Aklilu, Y., Zhang, J., Wong, I., Hayden, K., Li, S., Kirk, J., Scott, K., Moran, M., Robichaud, A., Cathcart, H., Baratzedah, P., Pabla, B., Cheung, P., and Zheng, Q.: Estimates of acid deposition critical load exceedances for Alberta and Saskatchewan using GEM-MACH, *Atmos. Chem. Phys. Disc.*, doi:acp-2017-1094, 2018.
- 890 Makar, P. A., Zhang, J., Gong, W., Stroud, C., Sills, D., Hayden, K. L., Brook, J., Levy, I., Mihele, C., Moran, M. D., Tarasick, D. W., He, H., and Plummer, D.: Mass tracking for chemical analysis: the causes



- 895 of ozone formation in southern Ontario during BAQS-Met 2007, *Atmos. Chem. Phys.*, 10, 11 151–11 173, doi:10.5194/acp-10-11151-2010, 2010.
- Makar, P. A., Gong, W., Milbrandt, J., Hogrefe, C., Zhang, Y., Curci, G., Zabkar, R. ., Im, U., Balzarini, A., Baró, R., Bianconi, R., Cheung, P., Forkel, R., Gravel, S., Hirtl, M., Honzak, L., Hou, A., Jiménez-Guerrero, P., Langer, M., Moran, M., Pabla, B., Pérez, J., Pirovano, G., José, R. S., Tuccella, P., Werhahn, J., Zhang, J., 900 and Galmarini, S.: Feedbacks between air pollution and weather, part 1: Effects on weather, *Atmos. Environ.*, 115, 442–469, doi:10.1016/j.atmosenv.2014.12.003, 2015b.
- Menichini, E.: On-filter degradation of particle-bound benzo(a)pyrene by ozone during air sampling: a review of the experimental evidence of an artefact, *Chemosphere*, 77, 1275–1284, doi:10.1016/j.chemosphere.2009.09.019, 2009.
- 905 Miao, Q., Bouchard, M., Chen, D., Rosenberg, M. W., and Aronson, K. J.: Commuting behaviors and exposure to air pollution in Montreal, Canada, *Sci. Tot. Environ.*, 508, 193–198, doi:10.1016/j.scitotenv.2014.11.078, 2015.
- Moran, M., Menard, S., Gravel, S., Pavlovic, R., and Anselmo, D.: RAQDPS Versions 1.5.0 and 1.5.1: Upgrades to the CMC Operational Regional Air Quality Deterministic Prediction System Released in October 2012 and February 2013, Technical report, Canadian Meteorological Centre, Canadian Meteorological Centre, Dorval, Quebec, 2013.
- 910 Moran, M. D., Ménard, S., Talbot, D., Huang, P., Makar, P. A., Gong, W., Landry, H., Gravel, S., Gong, S., Crevier, L.-P., Kallaur, A., and Sassi, M.: Particulate-matter forecasting with GEM-MACH15, a new Canadian air-quality forecast model, in: *Air pollution modelling and its application XX*, edited by Steyn, D. G. and Rao, S. T., pp. 289–292, Springer, Dordrecht, 2010.
- 915 Mu, Q., Lammel, G., Gencarelli, C. N., Hedgecock, I. M., Chen, Y., Přibyllová, P., Teich, M., Zhang, Y., Zheng, G., van Pinxteren, D., Zhang, Q., Herrmann, H., Shiraiwa, M., Spichtinger, P., Su, H., Pöschl, U., and Cheng, Y.: Regional modelling of polycyclic aromatic hydrocarbons: WRF-Chem-PAH model development and East Asia case studies, *Atmos. Chem. Phys.*, 17, 12 253–12 267, doi:10.5194/acp-17-12253-2017, 2017.
- 920 Odabasi, M., Bayram, A., Elbir, T., Seyfioglu, R., Dumanoglu, Y., Bozlaker, A., Demircioglu, H., Altioek, H., Yatkan, S., and Cetin, B.: Electric Arc Furnaces for Steel-Making: Hot Spots for Persistent Organic Pollutants, *Environ. Sci. Technol.*, 43, 5205–5211, doi:10.1021/es900863s, 2009.
- Okochi, H., Sugimoto, D., and Igawa, M.: The enhanced dissolution of some chlorinated hydrocarbons and monocyclic aromatic hydrocarbons in rainwater collected in Yokohama, Japan, *Atmos. Environ.*, 38, 4403– 925 4414, doi:10.1016/j.atmosenv.2004.03.053, 2004.
- Pachón, J. E., Sarmiento, H., and Hoshiko, T.: Health risk represented by inhaling polycyclic aromatic hydrocarbons (PAH) during daily commuting involving using a high traffic flow route in Bogotá, *Rev. Salud Publica (Bogota)*, 3, 198–407, 2013.
- Pankow, J. F.: Review and comparative analysis of the theories on partitioning between the gas and aerosol particulate phases in the atmosphere, *Atmospheric Environment*, 21, 2275–2283, doi:10.1016/0004-6981(87)90363-5, 1987.
- 930 Pendlebury, D., Gravel, S., Moran, M., and Lupu, A.: The impact of chemical lateral boundary conditions in a regional air quality forecast model on surface ozone predictions during stratospheric intrusions, *Atmos. Environ.*, doi:10.1016/j.atmosenv.2017.10.052, 2017.



- 935 Pitts Jr., J., Paur, H.-R., Zielinska, B., Arey, J., Winer, A., Ramdahl, T., and Mejia, V.: Factors influencing reactivity of polycyclic aromatic hydrocarbons adsorbed on filters and ambient POM with ozone, *Chemosphere*, 15, 675–685, doi:10.1016/0045-6535(86)90033-0, 1986.
- Pöschl, U., Letzel, T., Schauer, C., and Niessner, R.: Interaction of ozone and water vapor with spark discharge soot aerosol particles coated with benzo[a]pyrene: O₃ and H₂O adsorption, benzo[a]pyrene degradation, and atmospheric implications, *J. Phys. Chem.*, 105, 4029–4041, 2001.
- 940 Ringuet, J., Albinet, A., Leoz-Garzandia, E., Budzinski, H., and Villenava, E.: Reactivity of polycyclic aromatic compounds (PAHs, NPAHs, and OPAHs) adsorbed on natural aerosol particles exposed to atmospheric oxidants, *Atmos. Environ.*, 61, 15–22, doi:10.1016/j.atmosenv.2012.07.025, 2012.
- Samaali, M., Moran, M., Bouchet, V., Pavlovic, R., Cousineau, S., and Sassi, M.: On the influence of chemical initial and boundary conditions on annual regional air quality model simulations for North America, *Atmos. Environ.*, 43, 4873–4885, 2009.
- 945 Sandeep, K., Crews, W., Zmud, M., Fujita, E., Burnette, A., Snow, R., Santos, R., Campbell, D., Fincher, S., Bricka, S., Arnott, P., and Sabisch, M.: Kansas City PM characterization study: Final Report, Report, Assessment and Standards Division, Office of Transportation and Air Quality, U.S. EPA, and the Eastern Research Group Inc., 5608 Parkcrest Drive Suite 100, Austin, TX, U.S.A., 2008.
- 950 Sander, R.: Modeling atmospheric chemistry: interactions between gas-phase species and liquid cloud/aerosol particles, *Surveys in Geophysics*, 20, 1–31, 1999.
- Schauer, C., Neissner, R., and Pöschl, U.: Polycyclic aromatic hydrocarbons in urban air particulate matter: decadal and seasonal trends, chemical degradation, and sampling artifacts, *Environ. Sci. Technol.*, 37, 2861–2868, doi:10.1021/es034059s, 2003.
- 955 Skrdlíková, L., Landlová, L., Klánová, J., and Lammel, G.: Wet deposition and scavenging efficiency of gaseous and particulate phase polycyclic aromatic compounds at a central European suburban site, *Atmos. Environ.*, 45, 4305–4312, doi:10.1016/j.atmosenv.2011.04.072, 2011.
- Smith, D. J. T. and Harrison, R. M.: Concentrations, trends and vehicle source profile of polynuclear aromatic hydrocarbons in the U.K. atmosphere, *Atmos. Environ.*, 30, 2513–2525, doi:10.1080/10962247.2015.1096863, 1996.
- 960 Stroud, C., Moran, M., Makar, P., Gong, S., Gong, W., Zhang, J., Slowik, J., Abbatt, J., Lu, G., Brook, J., Mihele, C., Li, Q., Sills, D., Strawbridge, K., McGuire, M., and Evans, G.: Evaluation of chemical transport model predictions of primary organic aerosol for air masses classified by particle component-based factor analysis, *Atmos. Chem. Phys.*, 12, 8297–8321, doi:10.5194/acp-12-8297-2012, 2012.
- 965 Thackray, C. P., Friedman, C. L., Zhang, Y., and Selin, N. E.: Quantitative Assessment of Parametric Uncertainty in Northern Hemisphere PAH Concentrations, *Environ. Sci. Tech. Lett.*, doi:10.1021/acs.est.5b01823, 2015.
- Umwelterhebungen und Gerätesicherheit: Ozone Cross-sensitivity by the Emission Measurements of Suspended-particles Accumulated Benzo(a)-pyrene, Umeg report no. 33-02-2002, english version, Assessment and Standards Division, Office of Transportation and Air Quality, U.S. EPA, and the Eastern Research Group Inc., Zentrum für Umweltmessungen. Umwelterhebungen und Gerätesicherheit, Karlsruhe, Germany, 2002.
- 970



Table 1. Original (from Jonker and Koelmans (2002)) and adjusted (based on AURAMS-PAH model-measurement analysis for North America) K_{SW} values.

| | PHEN | ANTH | FLRT | PYR | BaA | CHRY | BaP |
|--------------|--------|--------|--------|--------|--------|--------|--------|
| Original Ksw | 4.34E5 | 1.55E6 | 2.24E6 | 1.70E6 | 3.74E7 | 2.82E7 | 9.59E7 |
| Adjusted Ksw | 3.32E7 | 4.21E7 | 8.24E7 | 9.84E7 | 1.75E8 | 3.23E7 | 1.10E8 |

- US EPA: AP 42, Fifth Edition, Compilation of Air Pollutant Emission Factors, Volume 1: Stationary Point and Area Sources, Report, Office of Air Quality Planning and Standards, Office of Air and Radiation, Research Triangle Park, NC, 27711, USA, 1995.
- 975 U.S. EPA: Locating and estimating air emissions from sources of polycyclic organic matter, Report epa-454/r-98-014, U.S. EPA, OAQPS, Washington, DC, 1998.
- U.S. EPA: National Air Toxics Trends Stations quality assurance annual report calendar year 2009 - Final Report, Office of Air Quality Planning and Standards, Research Triangle Park, NC 27711, USA, 2009.
- 980 Wang, X., Zhang, L., and Moran, M.: Uncertainty assessment of current size-resolved parameterizations for below-cloud particle scavenging by rain, *Atmos. Chem. Phys.*, 10, 5685–5705, doi:10.5194/acp-10-5685-2010, 2010.
- Wania, R., Mackay, D., and Hoff, J. T.: The importance of snow scavenging of polychlorinated biphenyls and polycyclic aromatic hydrocarbon vapors, *Environ. Sci. Tech.*, 33, 195–197, doi:10.1021/es980806n, 1999.
- 985 Wesely, M. L.: Parameterization of surface resistances to gaseous dry deposition in regional-scale numerical models, *Atmos. Environ.*, 23, 1293–1304, doi:10.1016/0004-6981(89)90153-4, 1989.
- Whaley, C., Makar, P. A., Shephard, M. W., Zhang, L., Zhang, J., Zheng, Q., Akingunola, A., Wentworth, G. R., Murphy, J. G., Kharol, S. K., and Cady-Pereira, K. E.: Contributions of natural and anthropogenic sources to ambient ammonia in the Athabasca Oil Sands and north-western Canada, *Atmos. Chem. Phys. Discussions*, 2017, 1–38, doi:10.5194/acp-2017-627, 2017.
- 990 Xu, H.-Y., Zou, J.-W., Min, J.-Q., and Wang, W.: A quantitative structure–property relationship analysis of soot–water partition coefficients for persistent organic pollutants, *Ecotox. Environ. Safety*, 80, 1–5, doi:10.1016/j.ecoenv.2012.02.002, 2012.
- Yamasaki, H., Kuwata, K., and Miyamoto, H.: Effects of ambient temperature on aspects of airborne polycyclic aromatic hydrocarbons, *Environ. Sci. Technol.*, 16, 189–194, doi:10.1021/es00098a003, 1982.
- 995 Zhang, J., Wang, P., Li, J., Mendola, P., Sherman, S., and Ying, Q.: Estimating population exposure to ambient polycyclic aromatic hydrocarbon in the United States - Part II: Source apportionment and cancer risk assessment, *Environment International*, 97, 163–170, doi:10.1016/j.envint.2016.08.024, 2016.
- Zhang, J., Li, J., Wang, P., Chen, G., Mendola, P., Sherman, S., and Ying, Q.: Estimating population exposure to ambient polycyclic aromatic hydrocarbon in the United States - Part I: Model development and evaluation, *Environment International*, 99, 263–274, doi:10.1016/j.envint.2016.12.002, 2017.
- 1000 Zhang, L., Gong, S., Padro, J., and Barrie, L.: A size-segregated particle dry deposition 270 scheme for an atmospheric aerosol module, *Atmos. Environ.*, 35, 549–560, 2001.
- Zhang, L., Moran, M., Makar, P., Brook, J., and Gong, S.: Gaseous Dry Deposition in AURAMS A Unified Regional Air-quality Modelling System, *Atmos. Environ.*, 36, 537–560, doi:10.1016/S1352-2310(01)00447-2, 2002.
- 1005

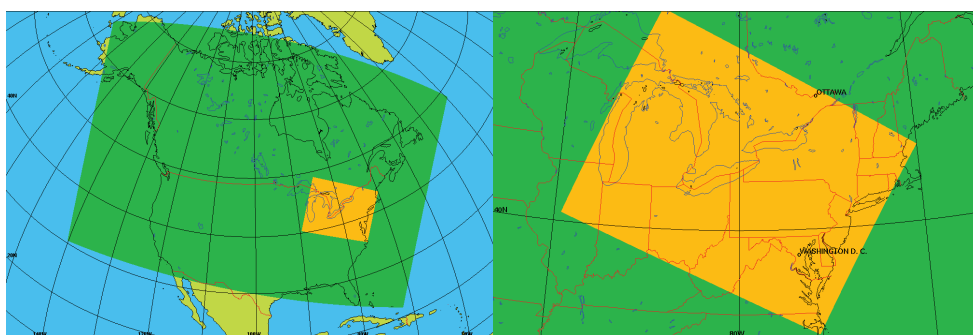


Figure 1. North American model domain with 10-km horizontal grid spacing (green), and the nested “Pan Am model” domain with 2.5-km horizontal grid spacing (orange).

Table 2. Mean and median GEM-MACH-PAH model/measurement ratios for PAH wet deposition

| | PHEN | ANTH | FLRT | PYR | BaA | CHRY | BaP |
|--------------|------|------|------|-----|------|------|------|
| mean ratio | 17.5 | 47.4 | 11.5 | 7.4 | 22.2 | 6.1 | 15.0 |
| median ratio | 8.1 | 10.5 | 8.5 | 5.4 | 17.9 | 6.4 | 10.3 |

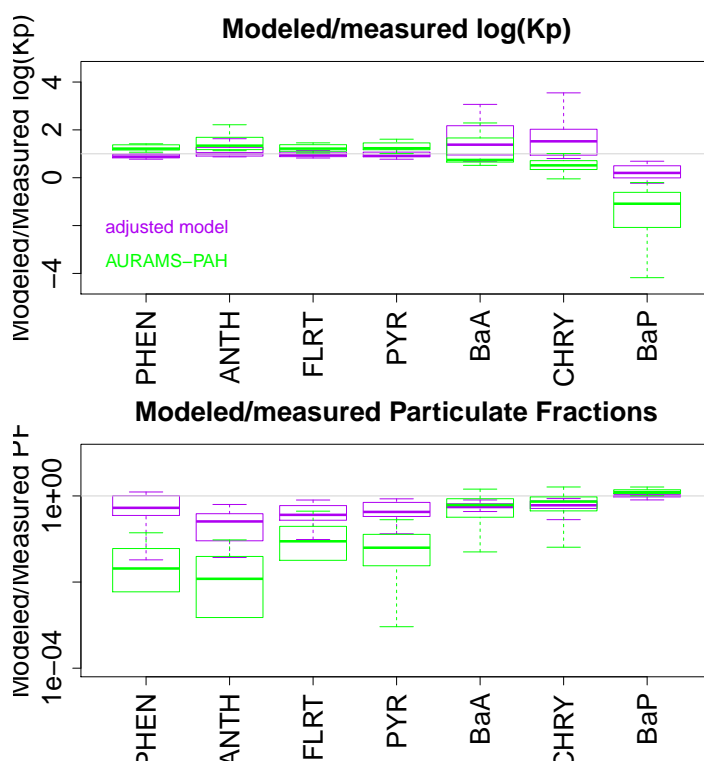


Figure 2. All-site ensemble of modeled/measured ratios of (top) log K_p , and (bottom) particulate fraction, for each PAH. Shown is the “adjusted model” (purple, from Eq. (B.2.1)), and the original AURAMS-PAH model (green). Box and Whiskers: thick line is the median, boxes extend to the 25th and 75th percentiles, and whiskers extend to the minimum and maximum.

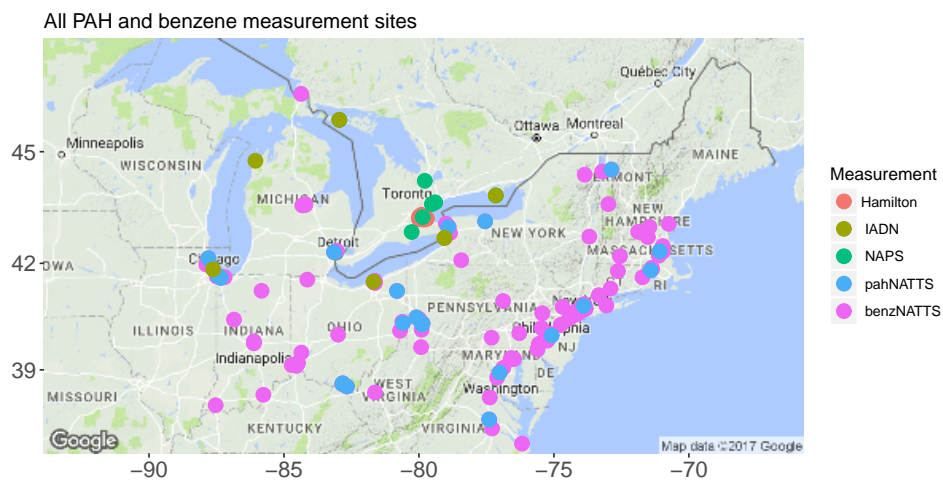


Figure 3. NAPS, NATTS, IADN and Hamilton measurement sites in the model domain.

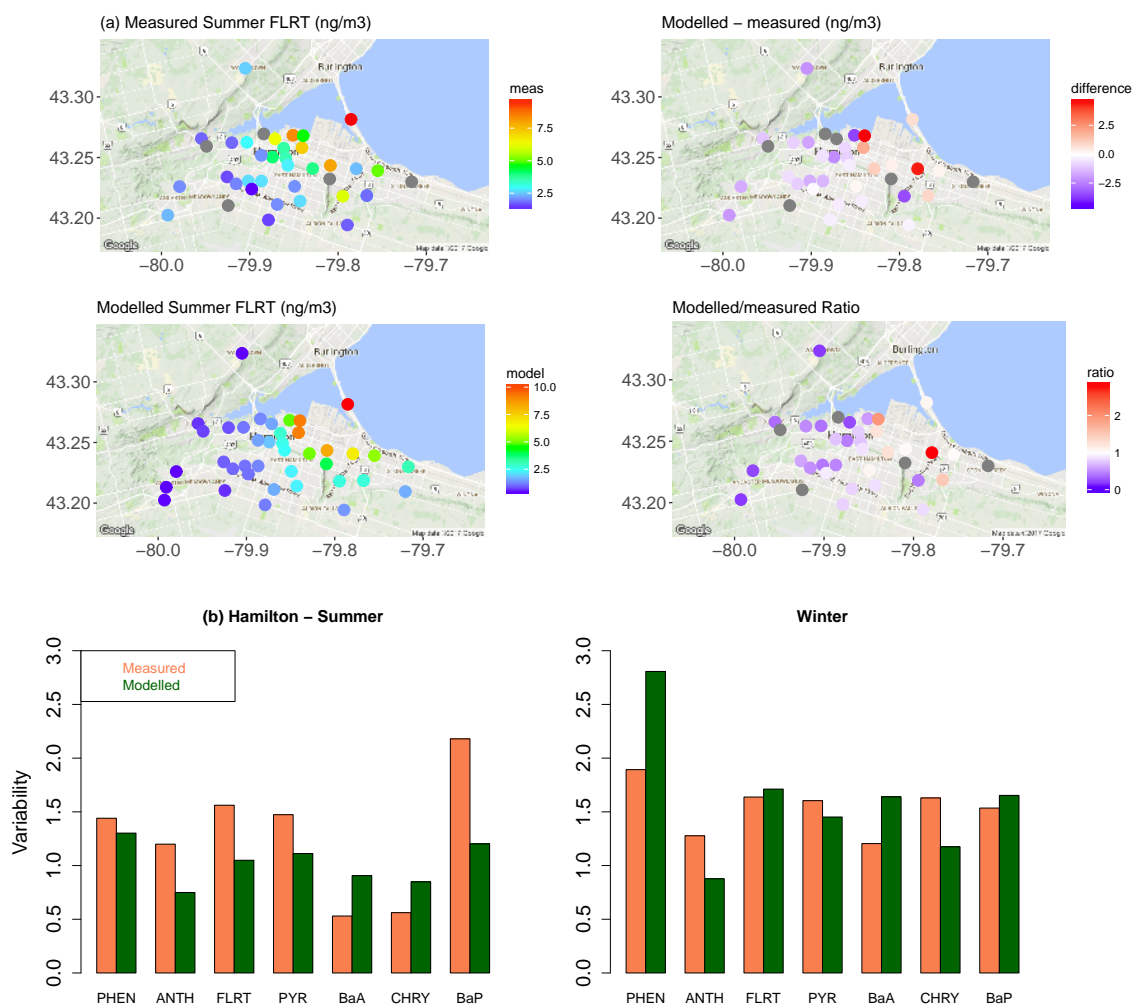


Figure 4. (a) Map of 2-week summertime average fluoranthene concentrations in Hamilton, Ontario: (left) from measurements and GEM-MACH-PAH model, and (right) their differences and ratios. (b) Spatial variability in the Hamilton data in (left) summer, and (right) winter.

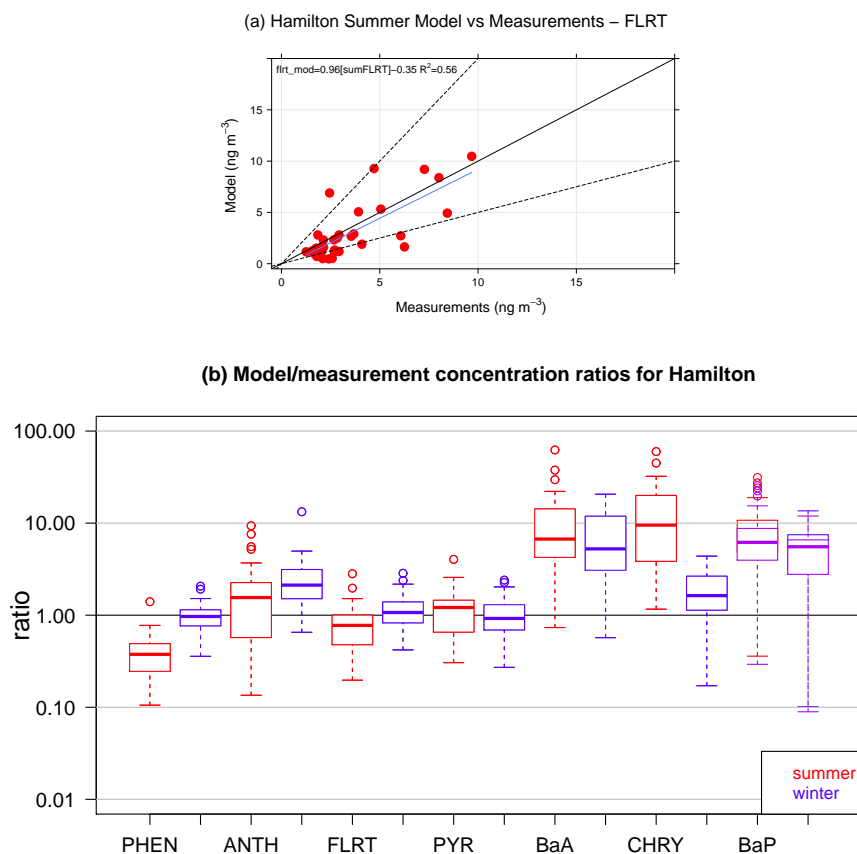


Figure 5. (a) GEM-MACH-PAH model vs. measurement scatter-plot of 2-week summertime fluoranthene concentrations at 40+ sites in Hamilton. (b) Frequency distributions of GEM-MACH-PAH model/measurement ratios of PAH concentrations for the Hamilton measurement-model pairs for all sites from both summer and winter. Purple boxes are results from O_3 -corrected BaP measurements.

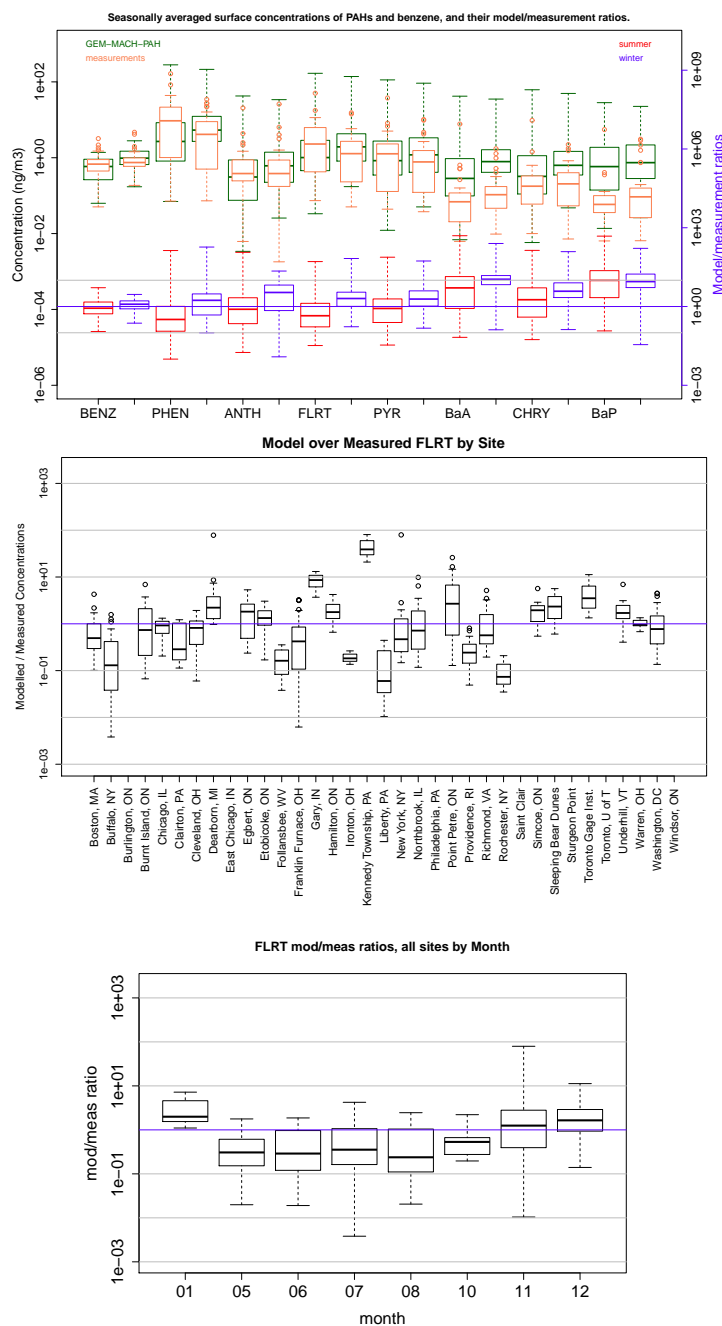
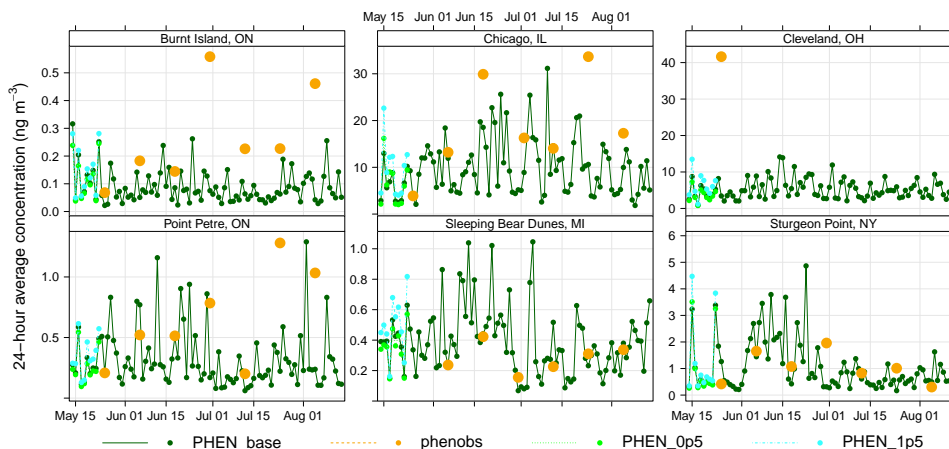


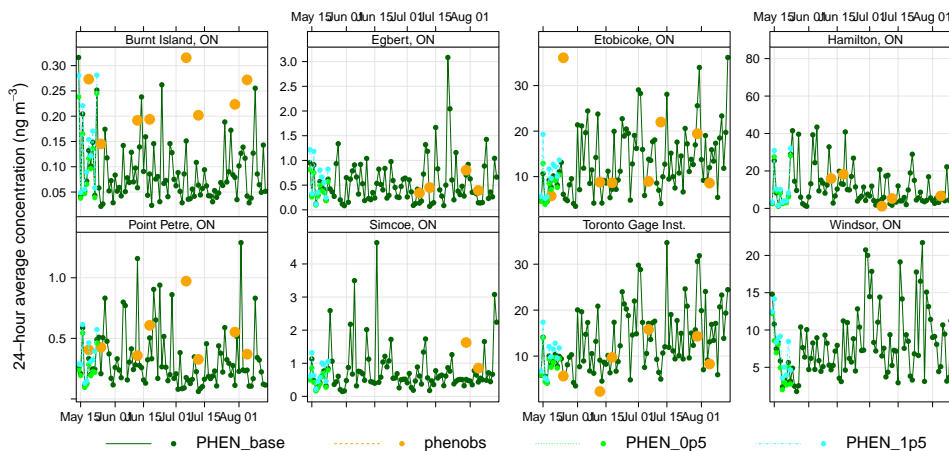
Figure 6. (a) Frequency distributions of GEM-MACH-PAH (green) and measured (orange) benzene (gas) and PAH (gas+particle) seasonal average concentrations at all IADN, NAPS, and NATTS sites. Modelled/measured concentration ratios also shown for summer (red) and winter (blue), with grey lines indicating agreement within an order of magnitude. (b) Modelled/measured concentrations for each daily model-measurement pair, separated by site (FLRT given as example), (c) same as (b) but separated by month.



PHEN (gas+particle) time series at IADN stations, Summer



PHEN (gas+particle) time series at NAPS stations, Summer



PHEN (gas+particle) time series at NATTS stations, Summer

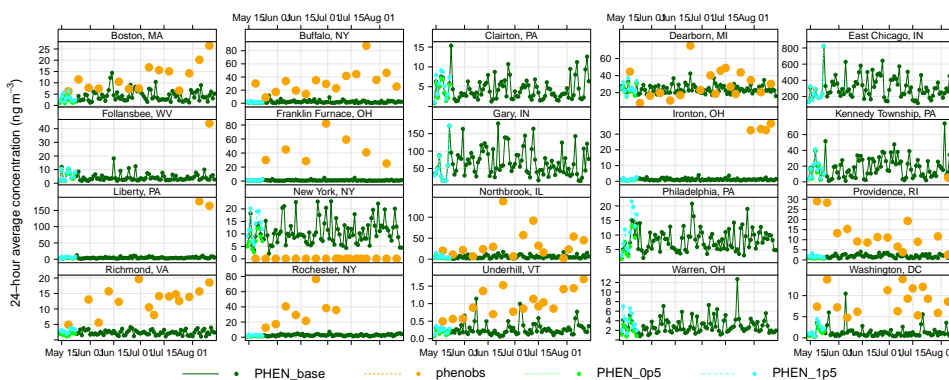


Figure 7. Phenanthrene time series for the summer 2009 period for the IADN (binational), NAPS (Canada) and NATTS (U.S.) networks. Orange=measurements, dark green=base GEM-MACH-PAH model, light green=GEM-MACH-PAH with 0.5×mobile emissions, cyan=GEM-MACH-PAH with 1.5×mobile emissions.

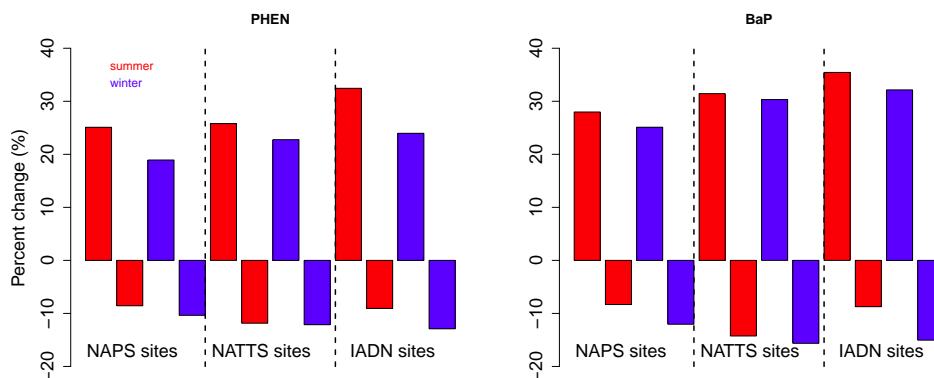


Figure 8. Average percent change in surface PHEN and BaP concentrations by season when PAH on-road mobile emissions are scaled up or down by factors of 1.5 and 0.5, respectively.

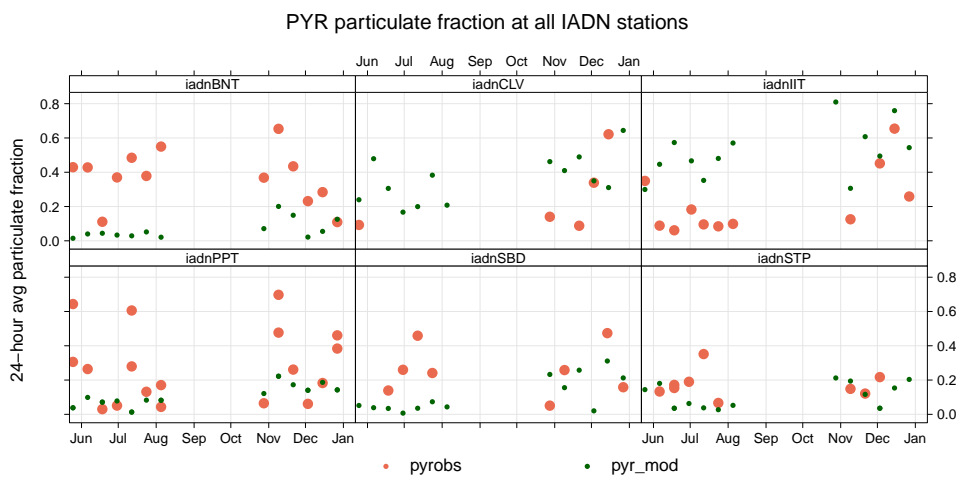


Figure 9. Time series of pyrene particulate fraction at six IADN network sites (BNT=Burnt Island, CLV=Cleveland, IIT=Chicago, PPT=Point Petre, SBD=Sleeping Bear Dunes, and STP=Sturgeon Point). GEM-MACH-PAH values are denoted by (green dots) and IADN measurements by orange dots.

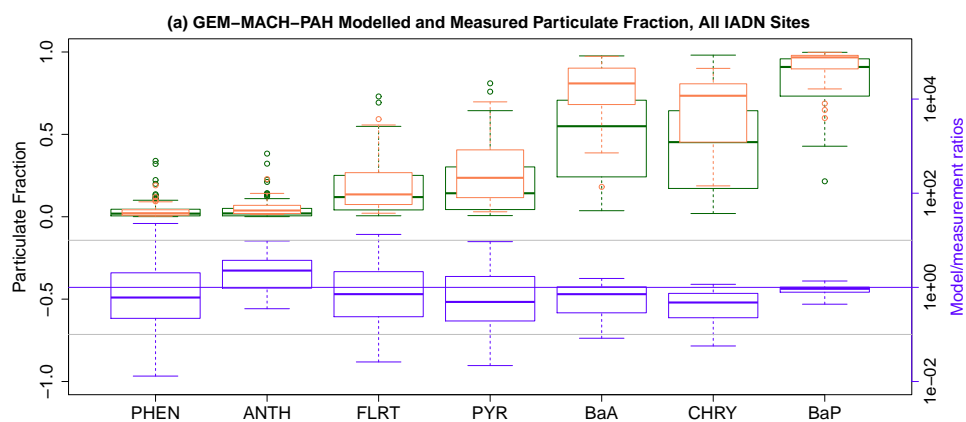


Figure 10. (a) GEM-MACH-PAH modelled (green) and measured (orange) particulate fraction (ϕ) of all PAHs at all IADN sites, and their model/measurement ratios. (b) Same as (a), but for partitioning coefficient ($\log K_p$). The blue line indicates the 1-to-1 line, and the gray lines are for ratios of 10 and 0.1.

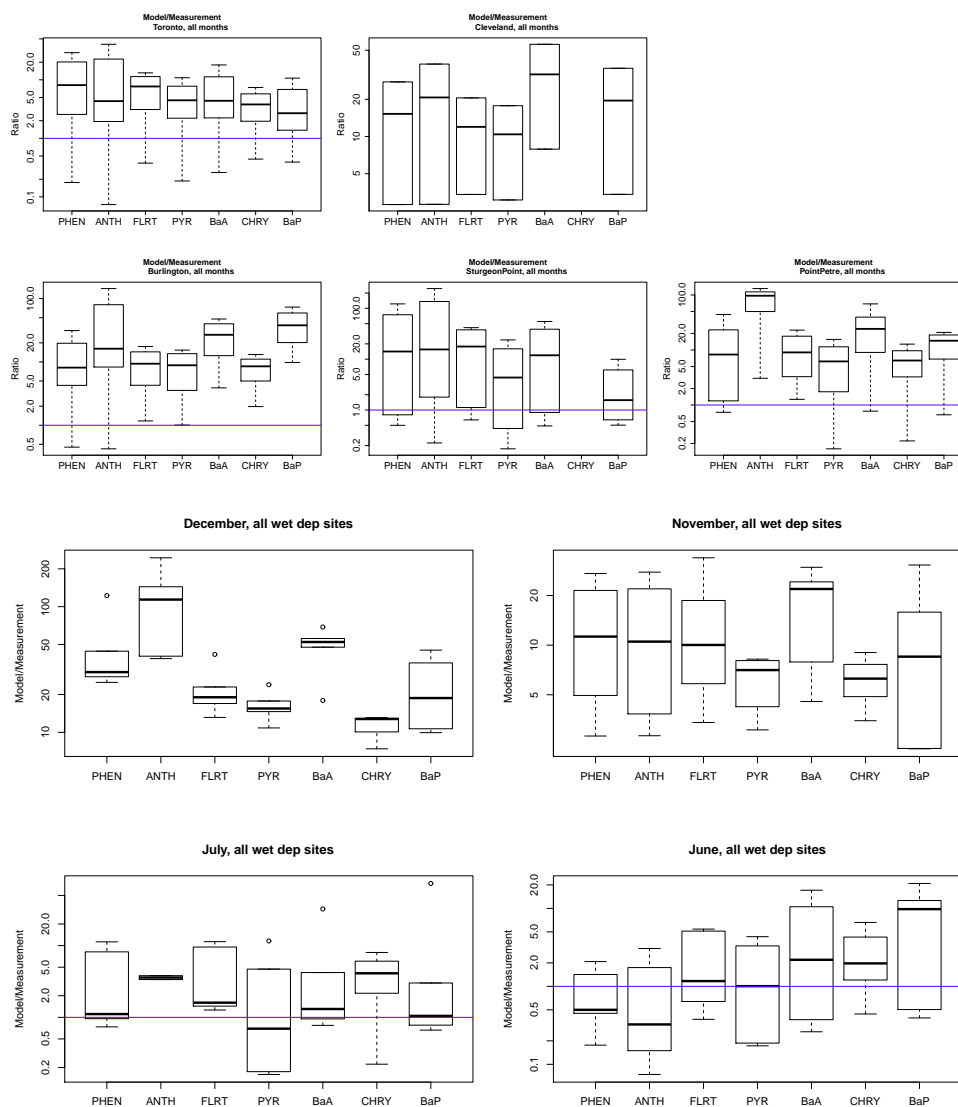


Figure 11. GEM-MACH-PAH model/measurement wet deposition ratios for all PAHs a) for five sites (all months) and b) for four months (all IADN sites).

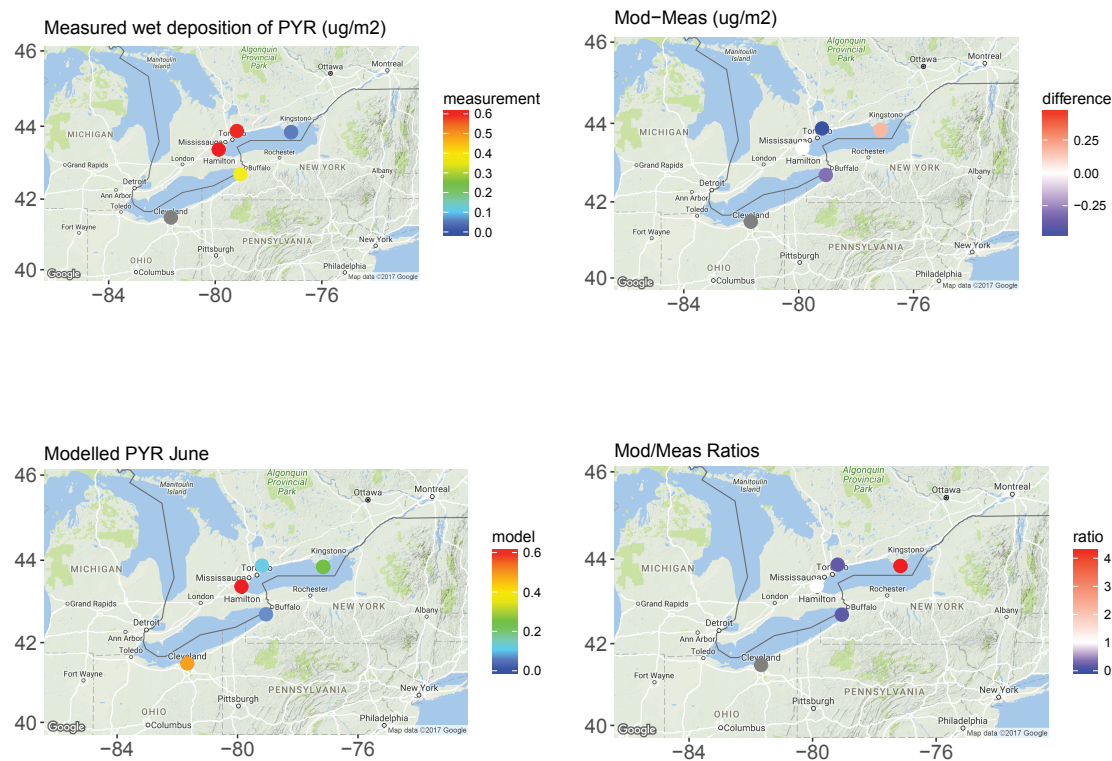


Figure 12. One-month (June 2009) wet deposition of pyrene from the (left) measurements and GEM-MACH-PAH model and (right) their differences and ratios.